BNWL-1522-2
UC-80

Battelle
Pacific Northwest Laboratories
Richland, Washington 99352

AEC Research and Development Report

TECHNICAL ACTIVITIES
QUARTERLY REPORT

AEC REACTOR DEVELOPMENT
AND TECHNOLOGY PROGRAMS

OCTOBER, NOVEMBER, DECEMBER 1970
JANUARY, FEBRUARY, MARCH 1971

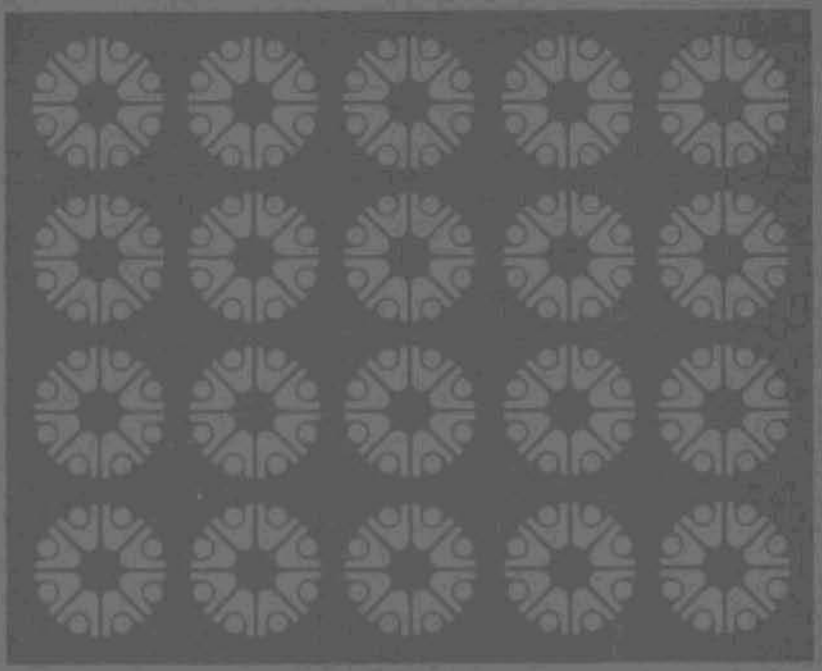

BNWL-1522-2

PACIFIC NORTHWEST LABORATORY
operated by
BATTELLE
for the
U.S. ATOMIC ENERGY COMMISSION
Under Contract AT(45-1)-1830

Printed in the United States of America
Available from
National Technical Information Service
U.S. Department of Commerce
5285 Port Royal Road
Springfield, Virginia 22151
Price: Printed Copy $3.00; Microfiche $0.95

BNWL-1522-2
UC-80
Reactor Technology

TECHNICAL ACTIVITIES QUARTERLY REPORT
AEC REACTOR DEVELOPMENT
AND TECHNOLOGY PROGRAMS
OCTOBER, NOVEMBER, DECEMBER 1970
JANUARY, FEBRUARY, MARCH 1971

By

Staff of Battelle-Northwest

Program Coordinator:
F. G. Dawson

June 1971

BATTELLE
PACIFIC NORTHWEST LABORATORIES
RICHLAND, WASHINGTON 99352

TECHNICAL ACTIVITIES QUARTERLY REPORT
AEC REACTOR DEVELOPMENT
AND TECHNOLOGY PROGRAMS
OCTOBER, NOVEMBER, DECEMBER 1970
JANUARY, FEBRUARY, MARCH 1971

FOREWORD

This report covers all programs except the Waste Studies Program conducted by the Pacific Northwest Laboratory for the U.S. Atomic Energy Commission's Reactor Development and Technology Division. The objective of the Technical Activities Quarterly Report is to inform the scientific community in a timely manner of the technical progress made on the programs. The report contains brief technical discussions of accomplishments in all areas where significant progress has been made during the reporting period. The results presented should be considered preliminary and do not constitute final publication of the work. A list of publications and papers is given in the report. Anyone wishing to obtain additional information on the work presented is encouraged to contact the author directly.

CONTENTS

1. SUMMARY

PLUTONIUM UTILIZATION PROGRAM

The ratio β_{eff}/ℓ (effective delayed-neutron fraction to prompt neutron lifetime) has been deduced from reactor noise measurements and compared to calculated values. The measurements have been made in a light-water-moderated and reflected lattice of half-inch diameter fuel rods containing UO_2 - 4 wt% PuO_2 . The measurements were made in the Plutonium Recycle Critical Facility in a lattice having a 1.06-inch square pitch.

A series of experiments with a 1.0-inch square light-water-moderated lattice containing UO_2 - PuO_2 fuel rods have been conducted in the Physical Constants Testing Reactor (PCTR) to measure the infinite neutron multiplication factor, k_∞, as a function of PuO_2 particle size. Experiment-theory correlation was completed for the k_∞ = 1 lattice compositions, in which the concentration of natural boron dissolved in the water moderator was adjusted experimentally to achieve a null-reactivity condition in the equilibrium neutron spectrum of the test lattice.

Infinite neutron multiplication factors and relative reaction rates have been measured in a water-moderated UO_2 - PuO_2 particle-size fuel lattice. Experiment-theory correlation of the results show that calculations consistently overestimate the infinite neutron multiplication factors for the unpoisoned lattice by three percent. Similar correlation of results for the lattice poisoned to k_∞ of unity has shown that calculations consistently underestimate infinite neutron multiplication factors by one percent.

Several problems relating to the licensing of recycle fuel are being studied. They are evaluations of the relative strength of PWR control clusters for UO_2 and PuO_2/UO_2 cores and evaluation of the Relative Hazard from Potential Release of radioactive materials from UO_2 and PuO_2/UO_2 cores.

A corrected ENDF/B-I description was developed following a review of experimental data on the total and scattering cross sections of deuterium. Calculations of neutron age using the corrected ENDF/B-I description gave better agreement with the experimental values. A manuscript of this review was submitted to the Cross Section Evaluation Working Group.

Plutonium fuels used in lattice experiments were analyzed destructively and nondestructively to check on fuel content and composition. Results of chemical analyses and gamma scanning for Al-Pu rods are reported. It appears that average plutonium enrichment values used over the years are valid.

A computer program called DRAFT is available to calculate fission product activities and activity ratios at selected times during and after irradiation. Program output (including plotting options) and utility are described.

The detailed postirradiation examination of selected fuel rods from the PRTR has been completed. A summary report describing the results is being prepared.

Detailed examination of four pins containing large PuO_2 particles in mixed-oxide pellet fuel after transient irradiation at SPERT shows that cladding penetration was caused by localized melting during the expulsion of molten or vaporized PuO_2 particles.

HIGH TEMPERATURE REACTOR PHYSICS PROGRAM

Some revisions to the correction terms used in the evaluation of k_∞ in PCTR and HTLTR experiments have been derived for both the poisoned and unpoisoned methods of measurements.

Modifications were recently made to the safety circuit at HTLTR to reduce the number of unscheduled scrams and thus reduce the number of times the four reactor safety blades were thermally cycled.

Inspection by camera and film of the VSR safety blades after their exposure to high temperatures and the frequent duty cycles during the first

experimental run since their modification has indicated that the expected deformation is small and acceptable.

Final values of $k_\infty(T)$ have been obtained for the first HTGR experiment performed in the HTLTR.

The experimental program to obtain $k_\infty(T)$ for the third HTGR lattice (ThO_2 - $^{233}UO_2$ -C) has begun in HTLTR. Measurements have been completed at temperatures of 20°C, 150°C, 300°C, and 555°C. Calculational results predict a total change in k_∞ between 20°C and 1000°C of about 32×10^{-3}.

Preparations for the first MSBR experiment in HTLTR are nearly complete, with the experimental planning finished, and about 45% of the fuel blocks loaded with fuel blend. Calculational results predict a total change in k_∞ between 20°C and 1000°C of about 43×10^{-3}.

Room temperature measurements on the MSBR mockup lattice have been completed in the HTLTR. These measurements include the flux mismatch, relative reaction rates in the central cell and copper poison, and reactivity measurements of various central cells and material samples.

Experiment planning, preparation of materials for fuel loading, and pre-experiment analysis were begun for the ThO_2 - PuO_2 HTGR experiment in the HTLTR. High exposure PuO_2 microspheres coated with pyrolytic carbon will be blended with ThO_2 and carbon and then loaded into graphite fuel blocks. A C/Pu atom ratio of 7500 and a C/Th atom ratio of 250 are nominal values for the loaded fuel blocks. This experiment should provide a satisfactory check on the calculational methods used in predicting the effect of plutonium loadings in an HTGR system.

A thermal cross section data tape has been derived from ENDF/B-II data for natural copper, ^{63}Cu, ^{65}Cu, ^{232}Th, ^{233}U, ^{234}U, ^{235}U, ^{236}U, ^{238}U, ^{239}Pu, ^{240}Pu, ^{241}Pu, ^{242}Pu, water, graphite, ^{14}N and ^{16}O, all in the format required by GRANIT. Epithermal cross-section data has been generated via ETOG for ^{12}C, Mo, Nb, Ni, Fe, Cr, ^{235}U, ^{238}U, ^{233}U, ^{232}Th, ^{239}Pu, ^{240}Pu and ^{241}Pu. Epithermal data was processed in GAM-I format.

The ENDF/F description of carbon was reviewed. It was found that neither Versions I nor II adequately described the cross section. A manuscript of the review was submitted to the Cross Section Evaluation Working Group.

PHOENIX STUDIES

A detailed evaluation of the methods used for the burnup calculation of the Phoenix experiment has been initiated. The calculated burnup slope is relatively insensitive to the approximations used in the burnup calculation. However, the calculated burnup slope has an uncertainty of 25% due to uncertainties in fission-product cross sections. The burnup slope also contains an uncertainty of 15% due to the method of calculating the ^{240}Pu cross section over the 1 eV resonance.

A total of 48 irradiated fuel plates from the MTR-Phoenix Core have been received from INC. Gamma scanning of these plates is in progress.

The five Pu flux wands from the MTR-Phoenix Core have been gamma scanned. Destructive analysis has been performed to yield isotopic data. Analysis of these data is in progress.

Analysis of data from the MTR experiments continues, and a final report is in preparation.

STEADY STATE AND TRANSIENT SUBCHANNEL CODE DEVELOPMENT AND DATA ANALYSIS

An interim version of COBRA-III will be useful for analysis of steady state and transient thermal hydraulic problems. Continuing improvements are being made. An interim report is in preparation on the current status of COBRA-III computer program development.

Design and fabrication of an experimental laser-Doppler velocimeter apparatus are completed. Data will be collected on the turbulent flow structure of single-phase flow in rod bundles so that correlations can be developed and used in subchannel computer programs.

PLUTONIUM CRITICALITY STUDIES

The first two series of critical experiments with undermoderated mixtures of PuO_2 - UO_2 have been completed and a third is in progress. The critical thickness of a Plexiglas-reflected slab infinite in two dimensions was determined to be 10.90 ± 0.04 cm for the 30 wt% plutonium-enriched-47.4 H/(Pu + U) fuel, and 11.56 ± 0.09 cm for the 14.62 wt% plutonium-enriched-30.6 H/(Pu + U) fuel. The reflected critical cube sizes for each of these fuels were, respectively, 30.60 ± 0.05 cm and 33.30 ± 0.17 cm on a side. The corresponding masses of plutonium were 3.21 ± 0.05 kg and 3.13 ± 0.05 kg respectively.

Criticality experiments are being performed with plutonium nitrate solutions homogeneously poisoned with gadolinium to provide data for establishing nuclear safety limits. The first series, with a plutonium concentration of 116 g Pu/ℓ containing 0 - 2.5 g Gd/ℓ, has been completed and data is presented. A second series will be made in the concentration range of 300 - 400 g Pu/ℓ.

Criticality data was taken to determine the effect of Raschig rings in plutonium nitrate solutions for use in establishing nuclear safety guidelines. Glass rings containing 1/2 and 4 wt% boron, and stainless steel rings containing 1 wt% boron, were used. Data are presented for a concentration range of 63 to 412 g Pu/ℓ. the KENO code was used to calculate k_{eff} for the experimental critical systems, assuming poison to be homogeneous. Calculations are in progress for heterogeneous systems to better describe the experimental system and determine effects of self-shielding within the Raschig rings.

CALCULATIONS OF POTENTIAL ENVIRONMENTAL RADIOLOGICAL CONSEQUENCES OF REACTOR ACCIDENTS

This study has been completed. A final report will be separately issued.

NUCLEAR GRAPHITE

The two compressive creep capsules operating at 550°C and 800°C were discharged from the reactor after receiving a fluence of about 6×10^{21} n/cm^2 ($E > 0.18$ MeV). The creep is shown to be linear with stress and of about the expected magnitude for these low fluences.

The radiolytic reaction of carbon monoxide and water vapor, highly diluted with high purity helium, is being investigated. As was previously found with the carbon dioxide - hydrogen system, the radiolytic yields as a function of temperature are significantly different from those of the undiluted gaseous mixture.

Large graphite bars irradiated in KE-Reactor have been discharged after a fluence of 3×10^{21} n/cm^2 ($E > 0.18$ MeV). Also the "cold-seeded" samples have been discharged from ETR. Measurements of sample dimensions and properties are underway.

Samples irradiated in ETR at temperatures from 800°C to 1400°C were discharged from the reactor in March. Measurement of samples is scheduled to begin in April.

Crystal lattice expansions have been derived as a function of temperature using the theoretical relationships of Riley. This will enable one to better obtain information on morphology of porosity in graphites as it relates to irradiation damage.

ATR PRESSURIZED WATER LOOP OPERATION AND MAINTENANCE

The AEC-RDT Richland Office has approved the phase-out of Pacific Northwest Laboratory (PNL) as operating contractor for the 1D-N loop.

2. PLUTONIUM UTILIZATION PROGRAM

β_{eff}/ℓ FOR A Pu-ENRICHED H_2O LATTICE CONTAINING WATER REGIONS

V. O. Uotinen, W. P. Stinson and S. P. Singh

The ratio β_{eff}/ℓ (effective delayed-neutron fraction to prompt neutron lifetime) has been deduced from reactor noise measurements and compared to calculated values. The measurements have been made in a light-water-moderated and reflected lattice of half-inch diameter fuel rods[1] containing UO_2 - 4 wt% PuO_2. The measurements were made in the Plutonium Recycle Critical Facility[2] in a lattice having a 1.06-inch square pitch.

Measurements were made with a uniform core of these rods and after water regions were introduced into the core. A small and large water region were formed by removing two and four fuel rods from the center of the core. Measurements were made in each case to determine how β_{eff}/ℓ changes when a water region is introduced into the core. These measurements comprise an extension of earlier work[3] in which β_{eff}/ℓ was measured for a number of uniform light-water lattices.

Values of β_{eff}/ℓ were deduced from power spectral density data which were obtained by frequency-analyzing signals from ion chambers located in the water reflector adjacent to the core. Because of the small size of the core (17 cm radius) the reactor noise was assumeed to be spatially independent, and thus not dependent on the distance from the water hole to the ion chambers. A function that describes the measured power spectral density (including effects of instrument attenuation at high frequencies) was fit to the data points using the least-squares fitting program LEARN.[4] This program can fit linear or nonlinear explicitly defined functions. It seeks the least-squares fit by treating mean-square misfit as a second-order Taylor's expansion and minimizing it with respect to all the unknown parameters of the function.

Values of β_{eff}/ℓ and ℓ were calculated with a two-dimensional perturbation theory code (PERT-V)[5] which uses standard perturbation theory expressions for these quantities. Direct and adjoint fluxes for the perturbation theory calculations were obtained from two-dimensional diffusion

theory calculations using the computer code 2DB.[6] Multigroup parameters for use in the diffusion and perturbation codes were obtained from cell calculations using the codes HRG-3[7] and BATTELLE-REVISED-THERMOS-I.[8] Calculations were performed using four, six and eight energy groups. The four-group scheme had a broad fast group (10 MeV - 11.7 keV) and allowed no distinction to be made between the spectra of prompt and delayed neutrons.

The results and conclusions of this experimental and calculational study are summarized below.

- The measured value of β_{eff}/ℓ changed from 89 ± 2 sec^{-1} for a uniform core, to 83 ± 2 sec^{-1} for a core with two fuel rods removed, to 77 ± 2 sec^{-1} for a core with four fuel rods removed.
- Calculated values of β_{eff}/ℓ (using an 8-energy group, modified H_2O cross-section model) agree with measured values to within ±5% in all cases.
- Calculated values of β_{eff}/ℓ using six energy groups are about 18% greater than values obtained using four groups; values obtained using eight groups are about 3% greater than values obtained using six groups; these changes are due primarily to changes in β_{eff}.
- Calculations using modified water cross sections for water within the core yielded values of β_{eff}/ℓ about 1.5% smaller than when using uniform water cross sections in reflector and core; these changes were due primarily to changes in ℓ.
- The calculated value of ℓ increases by 7.5% and that of β_{eff} decreases by about 2% between the uniform core and the core with four fuel rods removed. Thus, while the major change is in ℓ, the change in β_{eff} is not negligible, and should be considered when interpreting reactivity measurements in lattices containing water regions of various sizes.

References

1. *W. P. Stinson and J. H. Lauby, "Approach to Critical Experiments with UO_2 - 4 wt% PuO_2 - H_2O Lattices," BNWL-963, p. 3.31, Pacific Northwest Laboratory, (1969).*

2. *R. A. Bennett and L. C. Schmid, "Approach to Critical and Calibration Experiments in the Plutonium Recycle Critical Facility," HW-80206, General Electric Company, (July 1964).*

3. *V. O. Uotinen, J. H. Lauby, W. P. Stinson, and S. R. Dwivedi, "Reactor Kinetic Parameters of Lattices of Plutonium and Uranium in Water," Nucl. Sci. & Eng., 44, pp. 66-72, April, 1971.*

4. *B. H. Duane, "Maximum Likelihood Nonlinear Correlated Fields (BNW Program LIKELY)," BNWL-390, Pacific Northwest Laboratory, (1967), and G. D. Seybold, "User's Aid: Programs LEARN and LIKELY," BNWL-1057, Pacific Northwest Laboratory, (1969).*

5. *R. W. Hardie and W. W. Little, Jr., "PERT-V, A Two-Dimensional Perturbation Code for Fast Reactor Analysis," BNWL-1162, Pacific Northwest Laboratory, (1969).*

6. *W. W. Little, Jr., and R. W. Hardie, "2DB, A Two-Dimensional Diffusion Burnup Code for Fast Reactor Analysis," BNWL-640, Pacific Northwest Laboratory, (1968).*

7. *J. L. Carter, "HRG3: A Code for Calculating the Slowing-Down Spectrum in the P_1 or B_1 Approximation," BNWL-1432, Pacific Northwest Laboratory, (1970).*

8. *C. L. Bennett and W. L. Purcell, "BRT-I: Battelle-Revised-THERMOS," BNWL-1434, Pacific Northwest Laboratory, (1970).*

EXPERIMENT-THEORY CORRELATION OF PuO_2 PARTICLE SIZE REACTIVITY EFFECT

D. F. Newman and C. R. Gordon

The ability to predict the effect that plutonium particle size has on the reactivity of a reactor system is important for reactor safety and economic utilization of plutonium. A series of experiments with a 1.0-inch square, light-water-moderated lattice containing UO_2 - PuO_2 fuel rods have been conducted in the Physical Constants Testing Reactor (PCTR) to measure the infinite neutron multiplication factor, k_∞, as a function of PuO_2 particle size. This data serves as a benchmark to which calculated values for k_∞, using theoretical methods which allow dilute granular composite fuel regions, can be compared. Experiment-theory correlation was completed for the $k_\infty = 1$ lattice compositions, in which the concentration of natural boron dissolved in the water moderator was adjusted experimentally to achieve a null-reactivity condition in the equilibrium neutron spectrum of the test lattice.

Poisoned Lattice Results

Calculations were made for each PuO_2 particle size fuel composition and boron concentration which achieved the null-reactivity condition ($k_\infty = 1$) in the PCTR, using the GRANIT[1] code for thermal group constants and the EGGNIT[2] code for epithermal group constants. A two-dimensional (R-Z) calculational model of the PCTR with the water moderated lattice installed in the test cavity, was used to evaluate small corrections to the null-reactivity boron concentrations due to neutron spectrum mismatch in the center cell and flux gradients between the radial buffer and center cell. These refinements, calculated using the 2DB[3] code, have resulted in small changes in the measured boron concentrations reported previously.[4] The revised boron concentrations, and results of the experiment-theory correlation for the poisoned lattice are listed in Table 2.1.

The relative plutonium enrichment in each type fuel was determined from extensive gamma scan measurements with a high resolution GeLi detector. Corrections were made for the difference in gamma ray attenuation due to lumping the plutonium in different diameter spherical particles.[5] One rod containing zero-micron PuO_2 particles and one rod containing 328-micron PuO_2 particles were dissolved and chemically analyzed.[6] The relative enrichment results were normalized to the chemical analysis data to obtain the percent by weight of PuO_2 in $UO_2 + PuO_2$ for each set of rods listed in Table 2.1.

Discussion and Conclusions

The uncertainty in the plutonium enrichment values is estimated at ±0.04 wt% PuO_2, which corresponds to a change in k_∞ in the poisoned lattice of ±0.004. This uncertainty in k_∞ is equal to the root-mean-square deviation of the average value calculated for k_∞ using measured null-reactivity boron concentrations, in the GRANIT-EGGNIT calculation, given in Table 2.1. The uncertainty in the boron concentrations in the water at $k_\infty = 1$ is estimated at ±4 weight-parts-per-million, which corresponds to a change in k_∞ of ±0.0007. Thus, the effect of PuO_2 particle size on reactivity in the poisoned lattice is calculated within the statistical uncertainty of the measured change in reactivity as a function of PuO_2 particle size. However,

TABLE 2.1. PuO_2 Particle Size Experiment-Theory Comparison

Fuel Type	PuO_2 Particle Diameter (microns)	Fuel Density gm/cm^3	wt% PuO_2 $UO_2 + PuO_2$	Experimental Boron Concentration in H_2O for $k_\infty = 1.000$	Calculated k_∞ at $k_\infty = 1.000$ Boron Concentration From Experiment
8BMB	0	8.571	1.98	1213 wppm	0.9903
8SC	0	8.704	2.06	1286	0.9894
8BME	0	8.474	2.11	1274	0.9933
8P50	52	8.601	2.29	1350	0.9905
8B100	107	8.739	2.43	1378	0.9923
8P100	107	8.638	2.43	1332	0.9988
8LD100	107	7.630	2.45	1227	0.9949
8B200	195	8.718	2.36	1275	0.9856
8P200	195	8.657	2.38	1261	0.9893
8B350	328	8.691	2.42	1163	0.9863
8RA350	328	8.798	2.49	1229	0.9841

Average Value = 0.9904

Root-Mean-Square Deviation = ±0.0041

the calculated values for k_∞ are consistently lower than the measured values by approximately one percent. Previous thermal disadvantage factor measurements in PCTR water moderated lattices[7] have shown that THERMOS and GRANIT calculations overestimate the flux in the moderator relative to the fuel. A similar result for this experiment could explain the difference between measured and calculated values for k_∞. An increase in the absorption rate in boron due to an overestimate of the flux in the moderator would result in lower calculated values for k_∞.

The reactivity effect due to PuO_2 particle size was calculated for the unpoisoned lattice using GRANIT-EGGNIT. A fuel density of 8.66 gm/cm^3 and a plutonium enrichment of 2.0 wt% PuO_2 were held constant as the PuO_2 particle size was varied from zero to 328-microns in diameter. Results of these k_∞ versus PuO_2 particle size calculations are shown in Figure 2.1. A reactivity increase of 55 milli-k is predicted for fuel containing 350-micron PuO_2 particles relative to fuel containing zero-micron PuO_2 particles (solid solution). This is a significant effect which must be taken into account for reactor safety and economic utilization of plutonium.

Experiment-theory correlation of the unpoisoned lattice k_∞ versus PuO_2 particle size data is completed. Foil perturbation effects on measured relative reaction rates have been evaluated using the DOTSN[8] code. Using calculated corrections to k_∞ for enrichment and fuel density differences between different sets of fuel rods, the PuO_2 particle size reactivity effect will be determined for the unpoisoned 1.0-inch water lattice fueled with UO_2 - 2.0 wt% PuO_2 rods.

References

1. *C. L. Bennett, "GRANIT: A Code for Calculating Position Dependent Thermal Neutron Spectra in Doubly Hetergeneous Systems by the Integral Transport Method," BNWL-1522-1, pp. 2.48 - 2.51, Technical Activities Quarterly Report, AEC Reactor Development and Technology Programs, July, August, September 1970, Pacific Northwest Laboratory, (October 1970).*

2. *C. R. Richey, "EGGNIT: A Multigroup Cross-Section Code," BNWL-1203, Pacific Northwest Laboratory, (November 1969).*

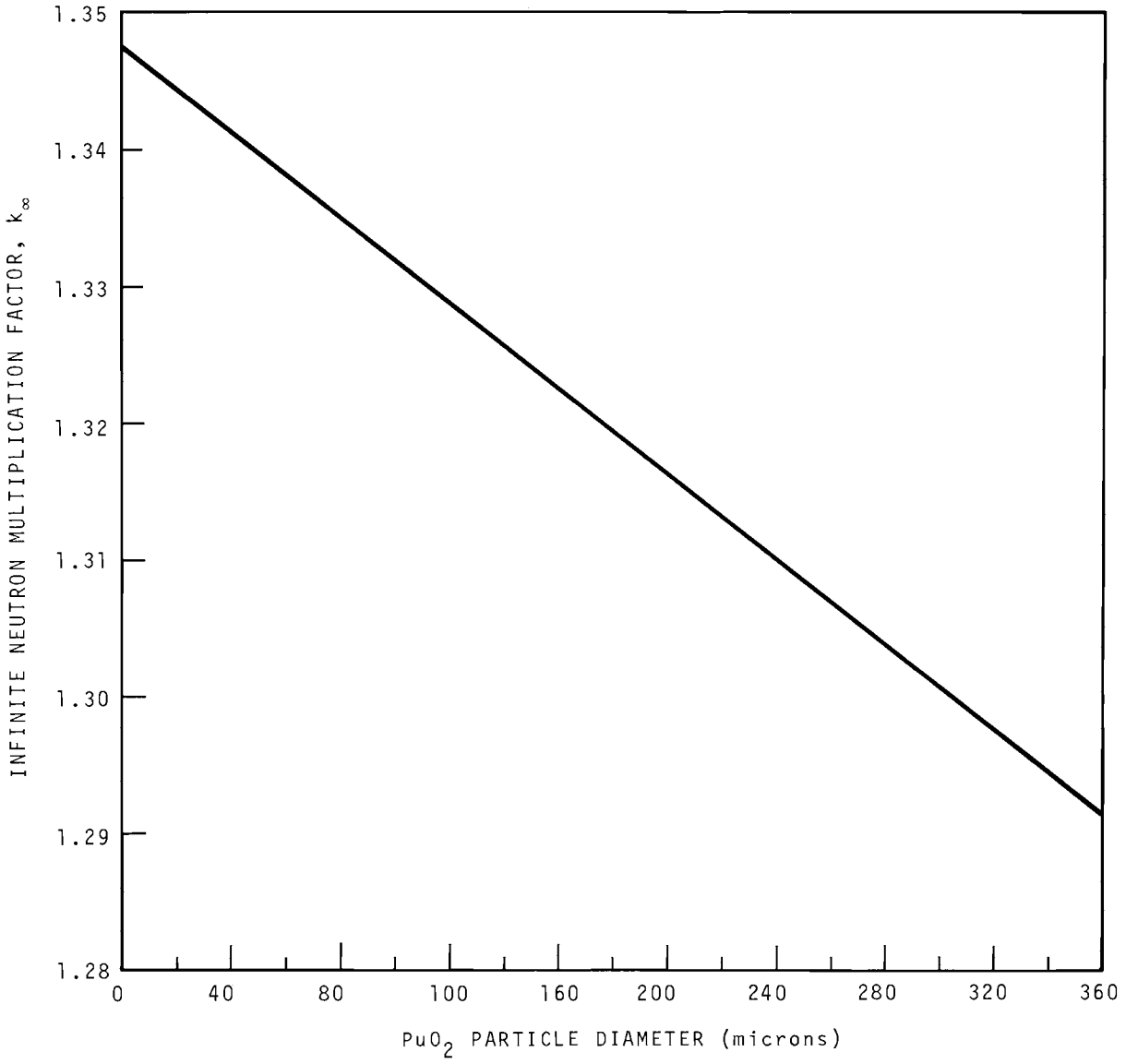

FIGURE 2.1. Calculated k_∞ Versus PuO_2 Particle Size

3. *W. W. Little, Jr., and R. W. Hardie, "2DB: A Two-Dimensional Diffusion Burnup Code for Fast Reactor Analysis," BNWL-640, Pacific Northwest Laboratory, (October 1966).*

4. *D. F. Newman and C. R. Gordon "PuO_2 Particle Size Reactivity Effect," BNWL-1522-1, pp. 2.43 - 2.47, Technical Activities Quarterly Report AEC Reactor Development and Technology Programs, July, August, September 1970, Pacific Northwest Laboratory, (October 1970).*

5. *Theodore Rockwell III, Editor, "Effect of Geometry of Radiation Source," p. 368, Reactor Shielding Design Manual, D. Van Nostrand Company (1956).*

6. *W. Y. Matsumoto, "Results of Analysis of UO_2 - PuO_2 Fuel Rod Specimens," Personal Communication, March 25, 1970.*

7. *D. F. Newman and D. R. Oden, "PCTR Measurement of k_∞ for UO_2 - 0.9 wt% PuO_2 Rods in 1.0-inch Square Pitch, Water Moderated Lattice," BNWL-739, pp. 3.21 - 3.34, Plutonium Utilization Program Technical Activities Quarterly Report, December 1967, January, February 1968, Pacific Northwest Laboratory, (April 1968).*

8. *F. R. Maynatt, "Users Manual for DOT," K-1694, Union Carbide Company, Oak Ridge, Tennessee.*

MEASUREMENT OF k_∞ AND RELATIVE REACTION RATES IN AN H_2O MODERATED UO_2 - PuO_2 PARTICLE SIZE FUELED LATTICE

D. F. Newman

Introduction

A series of experiments with a 1.0-inch-square, light-water-moderated lattice containing UO_2 - PuO_2 fuel rods has been conducted in the Physical Constants Testing Reactor (PCTR). These experiments provide reactivity and relative reaction rate data as a function of PuO_2 particle size distributed throughout the natural UO_2 diluent in 0.5-inch-diameter, zircalloy clad, fuel rods. Reactivity and relative reaction rate data provide a base for assessing the accuracy of calculational techniques used in reactor design to predict neutronic characteristics of light-water-moderated UO_2 - PuO_2 lattices.

PCTR Experiments

PCTR experiments utilize a small central test lattice region in which the neutron spectrum can be adjusted to duplicate the equilibrium spectrum in the fundamental mode (a just-critical, bare sphere of the test material). These experiments permit neutronic parameters of various reactor lattices to be measured using relatively small volumes of those lattices.[1] A removable central cell is surrounded both radially and axially by test lattice medium which is identical to the central cell and which brings the neutron spectrum into equilibrium. When the test lattice region is of sufficient volume, the neutron spectrum in the vicinity of the central cell is identical to the fundamental mode spectrum of the test lattice.[2]

The PCTR technique for measuring the infinite neutron multiplication factor, k_∞, of a multiplying medium is based upon the determination of the excess neutron production of a test sample.[3] This excess neutron production is deduced from the measured concentration of neutron absorber that must be added to the central test lattice region such that the change in the PCTR reactivity is zero when the central cell is removed, leaving a void.

The values of k_∞ measured in the PCTR were interpreted consistently with the theory used for fundamental mode calculations.[3] The expression used to evaluate the experimental k_∞ values for the unpoisoned lattice is

$$k_\infty = \frac{TP}{A_2}\left(\frac{A_2' + A_{2a}'}{TP'}\right)_{p'} - \frac{\left(1 + \tau B^2\right)\left(1 + L^2B^2\right)\left(1 - p\right)L^2B^2}{1 + \left(1 - p\right)L^2B^2} \quad . \qquad (1)$$

where,

TP = Total production rate of fast neutrons due to fission

A_2 = Absorption rate of thermal neutrons (E_n < 0.683 eV)

p = escape - to - thermal probability

The primed symbols refer to quantities in the poisoned lattice, and the term A_{2a}' is the thermal neutron absorption rate in the boron absorber added to the lattice moderator to produce null-reactivity.

Relative Reaction Rates

Foil activation techniques were utilized in the determination of the relative reaction rates in all central cell constituents and the standard absorber (usually copper) inserted in the center of the PCTR. Both bare and cadmium covered foils were used to measure epithermal - to - thermal reaction rates in the fuel, moderator, and cladding for all central cell constituents. The excess neutron production in the unpoisoned lattice can be determined from a neutron balance in the center cell, using the measured relative reaction rates after corrections due to foil perturbation effects[4] have been applied to the data.

Experiment Analysis

The presence of plutonium, which has a thermal neutron cross section with a significantly non - 1/v energy dependence, required a two-group expression for analysis of experimental data. The first term in Equation (1) is the dominant term. Relative reaction rates measured in the unpoisoned lattice were used to evaluate the quantity (TP/A_2). Similarly, the measured concentration of boron in the water corresponding to a k_∞ of unity and relative reaction rates measured in the poisoned lattice were used to evaluate the quantity

$$\frac{A_2' + A_{2a}'}{TP} \quad .$$

The addition of boron absorber in the water moderator did not change the slowing properties of the lattice significantly. The ratio of escape - to - thermal probabilities (p/p') was nearly unity. Values for (p/p') of 1.0125 for the UO_2 - 2.0 wt% PuO_2 lattice, and 1.0022 for the UO_2 - 0.9 wt% PuO_2 lattice were calculated using the HRG[5] code. The second term in Equation (1) is a small correction term to account for the fact that neutrons absorbed before being thermalized do not undergo thermal leakage. This term was evaluated as 0.0054 for the UO_2 - 2.0 wt% PuO_2 lattice and 0.0016 for the UO_2 - 0.9 wt% PuO_2 lattice, using thermal group parameters calculated using HGR. The fundamental mode buckling, B^2, was evaluated using THERMOS[6] and epithermal group parameters calculated using HRG. The fundamental mode buckling, B^2, was evaluated using the calculated two-group parameters for the unpoisoned lattice

$$B^2 = \frac{\eta_1 f_1 \left(1 - p\right) + \eta_2 f_2 \; p\text{-}1}{\tau + L^2 \; 1 - \eta_1 f_1 \left(1 - p\right)} \qquad (2)$$

where,

$$\eta_i f_i = \frac{\nu_i \Sigma_{f_i}}{\Sigma_{a_i}} \quad .$$

Similar quantities were calculated for the lattice with UO_2 - PuO_2 particle size fuel. Thermal group parameters were calculated using GRANIT[7] and epithermal group parameters were calculated using EGGNIT.[8] These computer codes permit calculation of doubly heterogeneous systems, which the UO_2 - PuO_2 particle size fuel lattice present. Experimental and calculated values for k_∞ in the unpoisoned lattice for various fuel types are listed in Table 2.2. Quantities used in the evaluation of experimentally derived values of k_∞ are also listed in Table 2.2.

The ability to predict the effect that plutonium particle size has on the reactivity of a reactor system is important for reactor safety and economic utilization of plutonium. Experiment-theory correlation of the UO_2 - PuO_2 particle size fueled lattice, poisoned to k_∞ of unity, has shown that the GRANIT-EGGNIT calculations consistently underestimate infinite medium, neutron multiplication factors by one percent.[9] Similar correlation of the unpoisoned lattice with the same fuels, given in Table 2.2, shows that the GRANIT-EGGNIT calculations consistently overestimate the neutron multiplication factors by three percent.

References

1. *D. J. Donahue, D. D. Lanning, R. A. Bennett, and R. E. Heineman, "Determination of k_∞ from Critical Experiments with the PCTR," Nuclear Science and Engineering, 4, 297 (1958).*

2. *D. D. Lanning, "On the Theory of PCTR Experiments," BNWL-1053, p. 2.14, Pacific Northwest Laboratories, Richland, Washington, (May 1969).*

3. *E. P. Lippincott, C. R. Richey, and D. D. Lanning, "Definition of the Infinite Neutron Multiplication Factors Measured by the PCTR Poisoned and Unpoisoned Technique," BNWL-1240, p. 2.3, Pacific Northwest Laboratories, Richland, Washington, (November 1969).*

TABLE 2.2. PuO_2 Particle Size Experiment Analysis of Unpoisoned Lattice k_∞

Particle Size Fuel Type	PuO_2 Particle Diameter, microns	$\left(\frac{TP}{A_2}\right)$	$\frac{TP}{A_2' + A_{2a}'}$	$\left(\frac{P}{P'}\right)$	Experimental k_∞	Calculated k_∞	Ratio $\left(\frac{\text{Calculation}}{\text{Experiment}}\right)$
8BMB	0	1.685	1.292	1.011	1.314 ± 0.005	1.345	1.024
8SC	0	1.699	1.296	1.012	1.322 ± 0.005	1.353	1.023
8BME	0	1.699	1.296	1.012	1.321 ± 0.005	1.357	1.027
8P50	52	1.707	1.296	1.013	1.328 ± 0.005	1.364	1.027
8B100	107	1.707	1.299	1.013	1.326 ± 0.005	1.368	1.031
8P100	107	1.704	1.305	1.012	1.317 ± 0.005	1.367	1.038
8LD100	107	1.674	1.294	1.012	1.304 ± 0.005	1.363	1.045
8B200	195	1.667	1.275	1.012	1.318 ± 0.005	1.350	1.024
8P200	195	1.668	1.279	1.012	1.314 ± 0.005	1.351	1.028
8B350	328	1.619	1.255	1.011	1.299 ± 0.005	1.337	1.029
8RA350	328	1.630	1.254	1.011	1.310 ± 0.005	1.343	1.025

Average Value = 1.029

Root - Mean - Square Deviation = ±0.006

Vibrationally Compacted Fuels	Nominal PuO_2 Particle Diameter (Microns)						
UO_2 - 2.0 wt% PuO_2	25	1.717	1.307	1.013	1.325 ± 0.005	1.365	1.030
UO_2 - 0.9 wt% PuO_2	25	1.315	1.192	1.002	1.104 ± 0.004	1.105	1.001

4. *D. F. Newman, "An Improved Method for Calculating Foil Perturbation Effects," Nucl. Sci. Eng., 44 (2), 261 (1971).*

5. *J. L. Carter, "HRG3: A Code for Calculating the Slowing-Down Spectrum in the P_1 or B_1 Approximation," BNWL-1432, Pacific Northwest Laboratories, Richland, Washington, (June 1970).*

6. *C. L. Bennett and W. L. Purcell, "BRT-1: Battelle-Revised-THERMOS," BNWL-1434, Pacific Northwest Laboratories, Richland, Washington, (June 1970).*

7. *C. L. Bennett, "GRANIT: A Code for Calculating Position Dependent Thermal Neutron Spectra in Doubly Hetergeneous Systems by the Integral Transport Method," BNWL-1522-1, p. 2.48-2.51, Pacific Northwest Laboratories, Richland, Washington, (October 1970).*

8. *C. R. Richey, "EGGNIT: A Multigroup Cross-Section Code," BNWL-1203, Pacific Northwest Laboratories, Richland, Washington, (November 1969).*

9. *D. F. Newman and C. R. Gordon, "Experiment-Theory Correlation of PuO_2 Particle Size Reactivity Effect," BNWL-1522-2, Pacific Northwest Laboratories, Richland, Washington, (current quarterly).*

EVALUATION OF THE RELATIVE STRENGTH OF PWR CONTROL CLUSTERS FOR UO_2 AND PuO_2/UO_2 CORES

W. C. Wolkenhauer

Recycle of plutonium fuel in light-water reactors requires the solution of several problems related to the licensing of the recycle fuel. One of these problems is the possible decrease in control rod strength with introduction of plutonium as the enriching fuel. The light-water core is typically designed and optimized for UO_2 fuel. Whether the control system is adequate for PuO_2/UO_2 fuel is of interest to the licensing analyst.

A series of calculations were performed to compare the relative strength of a PWR control cluster for a typical UO_2 and a PuO_2/UO_2 core. A representative PWR reactor design was used.(1) The calculations were performed using the THERMOS,(2) HRG(3) and 2DB(4) computer codes. The results of these calculations are still being analyzed. Some preliminary conclusions can, however, be reported at this time.

The calculations performed included analysis of the reactor cold excess reactivity for a typical UO_2 core and its recycle PuO_2/UO_2 core.

Therefore, the reactor geometry in the two cases differed only in that the latter case was enriched with fissile Pu rather than ^{235}U. All other parameters, such as pitch, clad outer diameter, and control cluster design were preserved. Calculations of the rodded core reactivity were also included.

Thermal pin cell flux disadvantage factors were calculated with the THERMOS code. Thermal constants for the fuel and control mixtures were calculated in slab geometry by the THERMOS code using the flux disadvantage factors as input. The effect of one control pin on its neighboring control pin was assessed. Methods for obtaining converged solutions in the high thermal absorber region were developed. Epithermal constants for the fuel and control regions were calculated using the HRG code. Methods for accounting for epithermal flux depressions were developed.

A two-dimensional, zero leakage diffusion calculation was performed on a typical fuel element geometry using the 2DB code. Cases calculated included the unrodded and rodded UO_2 and PuO_2/UO_2 cores. In addition, some cases were calculated to assess the effect of accelerated convergence of the final solution.

Preliminary analysis indicates that the PuO_2/UO_2 core exhibits about 70% of the reactivity control worth available to the UO_2 core with identical control geometry. This effect is attributed to the observed harder spectrum in the PuO_2/UO_2 core.

References

1. *SURRY Power Station Units 1 and 2, Final Safety Analysis Report, Virginia Electric and Power Company. 1969.*

2. *C. L. Bennett and W. L. Purcell, "BRT-I: Battelle-Revised-THERMOS," BNWL-1434. 1970.*

3. *J. L. Carter, "HRG3: A Code for Calculating the Slowing-Down Spectrum in the P_1 or B_1 Approximation." BNWL-1432. 1970.*

4. *W. W. Little, Jr. and R. W. Hardie, "2DB User's Manual," BNWL-831, Rev. 1. 1969.*

EVALUATION OF THE RELATIVE RADIOLOGICAL CONSEQUENCES FROM POTENTIAL RELEASE OF RADIOACTIVE MATERIALS FROM UO_2 AND PuO_2/UO_2 CORES

W. C. Wolkenhauer

A problem in licensing PuO_2/UO_2 cores is to determine if these kinds of cores represent a significantly greater potential radiological hazard than comparable UO_2 cores. If one can determine whether or not there are significant differences, then potential systems changes can be evaluated.

The integrated radiological burdens from a UO_2 PWR core and a comparable PuO_2/UO_2 PWR core were calculated for certain selected isotopes. The concentrations of these isotopes in curies/gm were calculated by use of the ALTHAEA[1] code for a typical exposure cycle. The relative potential radiological hazard was calculated by developing a parameter for each isotope which is defined as the total curies per gram for that exposure cycle divided by the Maximum Permissible Concentration (MPC) for that isotope. This parameter was then summed for each core and presented as a function of exposure.

The potential radiological hazard from PuO_2/UO_2 cores differs from that of UO_2 cores by the plutonium isotope inventory. Results of preliminary analyses indicate that the plutonium isotope inventory is significant and of the same order of magnitude as the fission product inventory in terms of the potential radiological hazard. It appears that even at extremely high exposures, the PuO_2/UO_2 cores will continue to exhibit a significantly higher potential radiological hazard. Additional work is being performed to substantiate these results.

Reference

1. *E. T. Merrill, "ALTHAEA: A One-Dimensional, Two-Group Diffusion Code With an Effective Four-Group Burnup," BNWL-462, (1969).*

REVIEW OF THE ENDF/B DESCRIPTION OF DEUTERIUM SCATTERING

B. R. Leonard, Jr.

All of the known experimental data on the total and scattering cross-sections of deuterium below 1.5 MeV were reviewed and compared with ENDF/B descriptions. The results of this review indicated that the knowledge of the deuterium cross-section below 0.5 MeV is clearly inadequate, culminating in a discrepancy of some 10% in the zero-energy value derived from the two most precise measurements. Review of the Version I description of ENDF/B revealed that the prescribed interpolation scheme created a cross-section which did not have the intended shape. Monte Carlo calculations of the neutron age in D_2O were carried out for the ENDF/B-I description with an improved interpolation and for the ENDF/B-II description, which differs from Version I only in the shape of the cross-section below 1.5 MeV. The calculated age with the corrected ENDF/B-I description was found to give better agreement with experimental values. A detailed manuscript of this review was submitted to the Cross-Section Evaluation Working Group.

DESTRUCTIVE AND NONDESTRUCTIVE ANALYSIS OF PLUTONIUM FUELS USED IN LATTICE EXPERIMENTS

W. P. Stinson and V. O. Uotinen

A series of critical and subcritical experiments have been performed to provide neutronic data on plutonium-fueled, light-water-moderated cores. These experimental data have been the base upon which the accuracy of neutronic reactor design methods have been evaluated. The results of criticality calculations for these cores have not compared very favorably with the measured results. As a part of the investigation aimed at uncovering the cause for these discrepancies, some of these fuels have been destructively analyzed to check on the fuel content and composition.

The plutonium-aluminum alloy fuels were examined in detail because these fuels were some of the first plutonium rods fabricated and thus were most suspect. One rod of each fuel type (Al-1.8 wt% Pu, Al-2 wt% Pu, and Al-5 wt% Pu) was sacrificed to perform:

- a chemical and an isotopic analysis for plutonium concentration and composition
- an alpha energy analysis for ^{241}Am content
- a spectrochemical analysis for detecting impurities (e.g., B, Cd and Au).

Two methods of destructively analyzing the fuel for plutonium content were used. These are the coulometric titration and isotopic dilution methods. Samples which were taken from the midpart of the fuel rods and from adjacent positions were analyzed.

The possibility of these Al-Pu rods having enrichment variation axially was investigated in a preliminary manner by gamma-ray scanning three unirradiated rods of each type.

The results of theory-experiment correlations for the Al-2 wt% Pu systems have been systematically different from those obtained for the other Al-Pu and UO_2 - PuO_2 systems. Therefore, a rod of this type was further analyzed for rare-earth isotopes and for hafnium content in the zircalloy cladding.

In addition to analyzing these Al-Pu fuels, two UO_2 - PuO_2 fuel rods were destructively analyzed for plutonium and americium content to determine how much ^{241}Pu had decayed. Repeat measurements were planned over a specified time period to assist in assessing the reactivity effect of ^{241}Pu decay.

Ten rods from each of three Al-Pu types of fuel were selected to represent the total batch of each. These ten rods bracketed the range of Pu content. The reactivity worth of each Al-Pu fuel rod was measured to obtain a basis for relating the results of the destructive analysis to the remainder of the fuel. These measurements were made in a central fuel channel in the PRCF. The core was UO_2 - 4 wt% PuO_2 (18% ^{240}Pu) fuel rods in an H_2O moderated lattice of 1.06-inch-square pitch. The lengths of the fuel rods are 43.83, 36.0, and 24.0 inches for the Al-1.8 wt% Pu, Al-2.0 wt% Pu, and the Al-5 wt% Pu, respectively. All the measurements were made with the fuel in a lucite thimble (1/32-inch wall thickness).

Results and conclusions obtained in this study are:

- On the basis of this study it appears that the average plutonium enrichments used in the past (e.g., BNWL-801) for these fuels are valid.
- The ^{241}Am content of these fuels was measured in March 1970. The results are listed in Table 2.3. These measured values can be used for determining the ^{241}Am content for experiments conducted with these fuels over the years.
- The rod-to-rod uniformity of each of the three types of Al-Pu rods is indicated by the results of the reactivity measurements given in Table 2.4. The Al-2 wt% Pu rods showed rather large variations, the standard deviation being 2 to 3 times as large for this fuel type than for the other fuel types.
- None of the impurities searched for were detected in the Al-Pu rods (down to a detection limit of 2 wppm).
- The axial uniformity measurements indicated some variations in enrichment might be present axially, but no conclusive statements can be made because the study was very limited.

TABLE 2.3. ^{241}Am Content of Fuel Rods, Measured March 1970

Rod Type	Fuel Diam., inches	Fuel Length, inches	$UO_2 - PuO_2$ or Al-Pu, grams/rod	^{241}Am, grams/rod
Al - 1.83 wt% Pu	0.500	43.83	389.3	0.0152
Al - 2.0 wt% Pu	0.500	36.0	318.2	0.0552
Al - 5.0 wt% Pu	0.500	24.0	219.9	0.0203
UO_2 - 2.0 wt% Pu (23.5% ^{240}Pu)	0.505	36.0	1128.0	0.229
UO_2 - 4.0 wt% PuO_2	0.4975	36.0	1084.5	0.279

TABLE 2.4. Uniformity of Al-Pu Rods

(Based on reactivity measurements of 10 rods of each type)

Rod Type	Average Reactivity Worth of a Rod, mk	Relative Standard Deviation of a Typical Rod	Relative Standard Deviation of Average
Al - 1.8 wt% Pu	1.271	2.7%	0.9%
Al - 2.0 wt% Pu	0.851	6.1%	2.0%
Al - 5.0 wt% Pu	2.691	2.1%	0.7%

DESCRIPTION OF PROGRAM DRAFT

D. R. Oden, T. M. Traver and G. D. Seybold

Program DRAFT calculates information concerning fission events such as fuel isotopic concentrations and fission product disintegration rates at selected times during and after irradiation. Irradiation history of the fuel is input in the form of a histogram to allow an accurate description of fission product formation. The following information is calculated and printed at as many as 100 values of time as specified by the user in the input through the power history.

- Accumulated exposure time
- Time averaged flux and accumulated exposure
- Fuel isotope (^{235}U, ^{238}U and ^{239}Pu) concentrations,
- Accumulated fissions in each fuel isotope (^{235}U, ^{238}U and ^{239}Pu), accumulated fissions in all fuel isotopes, and the fraction of accumulated fissions for each fuel isotope
- Disintegration rate for each fission product
- Ratios of selected fission product disintegration rates.

The above information can be generated for as many as 100 input exposure averaged fluxes, 20 fission products and 20 fission product activity ratios in a single pass. A plotting routine has been added to the program to allow for any or all of the following output to be plotted:

1. Ratio of final to initial fuel concentrations versus exposure.
2. Disintegration rate versus exposure or time, between any two specified times, for any fission product.
3. Disintegration rate ratio versus exposure or time between any two specified times and for any two fission products.

The code is used mainly for two purposes. First, it is used to determine which fission products and fission product activity ratios will be most useful in determining such quantities as average flux, exposure, fraction of fissions in each fuel isotope and total fissions for a particular reactor type. Secondly, the actual determination of these quantities is made by correlating the selected calculated fission product activity ratios with measured values obtained by nondestructive gamma scanning techniques.

PRTR FUEL EVALUATIONS

D. G. Carter and M. D. Freshley

With the shutdown of the PRTR, the irradiation performance of selected mixed oxide fuel rods irradiated in the reactor was evaluated by means of detailed destructive postirradiation examinations. The fuel evaluations included the following general fuel irradiation experiments conducted in the reactor:

- High Power Density Fuel Irradiations
- Extended Burnup Fuel Irradiations
- Internal Pressure Monitoring Experiment Rods
- FERTF Fuel Rods

The High Power Density (HPD) fuels were irradiated as part of the Batch Core Experiment. Most of the 66 HPD fuel elements irradiated were vibrationally compacted particle fuels, although pellet fuel fabricated by both the hot-press and the cold-press-sinter processes was included.

The extended burnup fuel irradiations included a variety of experimental UO_2 and UO_2 - PuO_2 elements containing 0.5, 1.0 and 2.0 wt% PuO_2. These elements were irradiated in fringe positions of the PRTR to evaluate the irradiation performance of the various fuel types subjected to extended burnups.

The PRTR fuel performance evaluations also included the detailed examination of mixed-oxide rods instrumented to monitor internal gas pressure buildup during irradiation. The comparative performance of mixed-oxide rods irradiated under identical conditions in the Fuel Element Rupture Test Facility (FERTF) in PRTR was also evaluated.

The detailed postirradiation examination phase of the PRTR fuel performance evaluation has been completed and a summary report describing the results is being prepared. Although the extent of examination varied considerably for individual rods the examination generally included the following:

- Visual examination for physical defects, crud deposition, corrosion, and fretting.
- Gamma scanning to determine axial power distribution, fuel movement, and axial fission product migration.
- Profilometer scanning to evaluate dimensional changes in the cladding such as ovality, swelling, and the effects of core-cladding interaction.
- Fission gas release.
- Burnup analysis by the cesium and/or neodymium methods.
- Fuel examination by optical and electron microscopy to evaluate structural changes and pore distribution. Beta-gamma and alpha autoradiography with electron microprobe analysis to evaluate PuO_2 homogeniety and plutonium and fission product migration.
- Cladding examination to assess zirconium-oxide formation on the internal and external clad surfaces, hydriding, and core-clad reaction.

A summary of the detailed examinations performed on selected individual HPD rods irradiated in PRTR is summarized in Table 2.5 and a summary of the detailed examinations performed on selected extended burnup fuel rods is presented in Table 2.6.

TABLE 2.5. Summary of PRTR High Power Density Fuel Rod Postirradiation Examination Status

Element Number	Rod No.	Fuel Type	^{148}Nd Peak Burnup, MWd/MTM	Gamma Scan	Profilometer Scan	Fission Gas Analysis	Burnup Analysis	Ceramography
6065	FE-74	UO_2 - 2 wt% PuO_2 (VP)	4863	X	O	X	X	O
	FO-17	(VP)	5837	X	O	X	X	O
	FS-07	(VP)	9176	X	X	X	X	O
6519	FR-72	(VP)	5240	X	X	X	X	X
	FN-86	(VP)	3297	X	O	X	X	X
	FE-69	(VP)	2884	X	O	X	X	X
6520	FR-78	(VP)	9630	X	X	X	X	X
6700	A-14	(HP)	8150	X	X	X	X	X
	A-103	(CPS)	3290	O	X	X	X	X
	A-102	(CPS)	3220	X	X	X	X	X
6701	A-23	(HP)	3430	X	X	X	X	X
	A-12	(HP)	3800*	O	X	X	O	X

(VP) = Vibrationally compacted, pneumatically impacted fuel
(CPS) = Cold-press-sinter pellet fuel
(HP) = Hot-press pellet fuel
X = Examination completed
O = Examination not performed
** = Estimated burnup value*

TABLE 2.6. Summary of the Postirradiation Examination Status for Fuel Rods Irradiated to Extended Burnup in PRTR Fringe Positions

Element Number	Rod No.	Fuel Type		^{148}Nd Peak Burnup, MWd/MTM	Gamma Scan	Profilometer Scan	Fission Gas Analysis	Burnup Analysis	Ceramography
1037	A-1330	UO_2	(SW)	12,079	X	0	X	X	X
	A-1377		(SW)	12,033	X	0	X	X	X
	A-1398		(SW)	15,368	X	0	X	X	X
	A-1325		(SW)	-	0	0	X	0	0
5118	DB-63	UO_2 - 0.5 wt% PuO_2	(VP)(MM)	18,500*	X	0	X	0	X
	DA-48		(VP)(MM)	18,500*	0	0	X	0	0
5186	ZZ-17		(CPS)	9,207	X	0	X	0	0
	ZZ-7		(CPS)	9,777	X	0	X	X	0
	ZZ-12		(CPS)	11,705	X	0	X	X	X
	CN-5		(SW)(MM)	12,500*	X	0	Lost	0	X
	CN-7		(SW)(MM)	12,500*	0	0	X	0	0
	CM-85		(SW)(MM)	12,500*	0	0	X	0	0
5224	CS-27	UO_2 - 1 wt% PuO_2	(SW)(PI)	13,500*	X	0	X	0	X
5226	DF-80		(VP)(PI)	11,500*	X	0	X	0	X
6003	5C-27	UO_2 - 2 wt% PuO_2	(VP)(PI)	13,000*	X	0	X	X	X
6005	5F-36		(SW)(PI)	7,180	X	0	X	X	X
6521	No. 6	ThO_2 - 5 wt% PuO_2	(VP)(PI)	Low	X	0	Lost	0	X

(VP) = Vibrationally compacted fuel
(SW) = Swage compacted fuel
(CPS) = Cold-press-sinter pellet fuel
(MM) = Heterogeneously enriched or incrementally loaded fuel material
(PI) = High-energy-rate pneumatically impacted fuel
X = Examination completed
0 = Examination not performed
** = Estimated burnup values*

TRANSIENT TESTING

M. D. Freshley, E. A. Aitken* and R. L. Johnson**

The behavior of oxide fuels when subjected to accidental high energy, short duration, power excursions is an important safety consideration in both thermal and fast reactors. Fuel performance under these conditions is important because the limiting design base accident for power reactors is established on the basis of maintaining fuel cladding integrity during a power excursion. A joint program involving Pacific Northwest Laboratory, General Electric Company, and Idaho Nuclear Corporation was conducted at SPERT to determine whether special considerations associated with adding PuO_2 enrichment to UO_2 could effect the transient behavior of mixed-oxide fuels. Emphasis was directed toward investigating the possible effects of large PuO_2 particles or agglomerates which may occur in mixed-oxide fuels when utilizing standard cold-press-sinter pellet fabrication techniques.

Four fuel pins containing 0.272-inch diameter enriched (7% ^{235}U) UO_2 pellets with a single PuO_2 microsphere embedded in alternate pellets in the 5.1-inch long fuel column were assembled in 0.020-inch thick Zircaloy-2 cladding with a nominal 0.004-inch diametral gap. The PuO_2 microspheres with a nominal diameter of 550 microns were strategically positioned within the pellets ranging from the center to the surface to investigate the possible influence of different spatial positions relative to the cladding. The Sol-gel PuO_2 microspheres retained their original appearance during the pellet fabrication although a shrinkage void appears to have formed between the PuO_2 microsphere and the UO_2 matrix during sintering (Figures 2.2 and 2.3).

Each of the four pins was subjected to a single transient power burst that resulted in adiabatic energy depositions of 189, 200, 213, and 237 cal/g of UO_2. A standard pin design was used to permit a comparison of the results from these tests with the results of other tests involving

---

* *General Electric Company*
** *Idaho Nuclear Corporation*

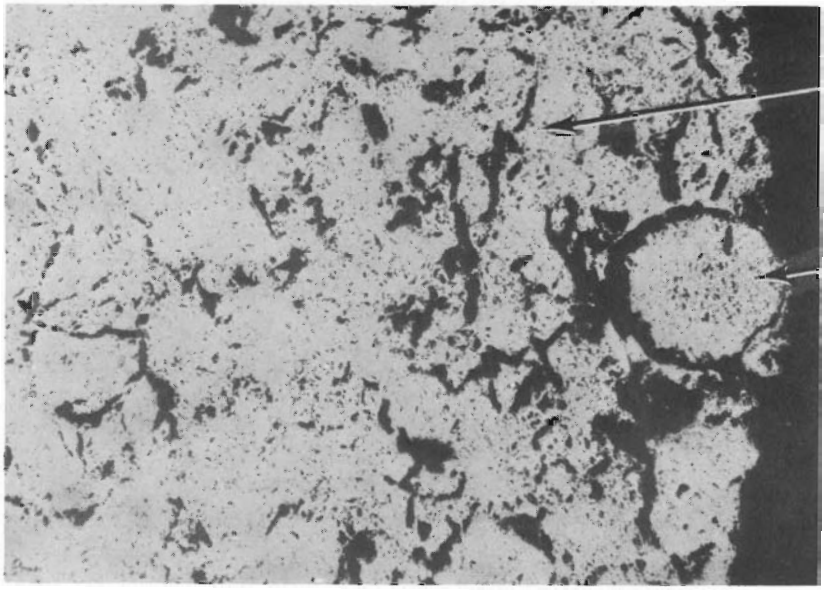

FIGURE 2.2. A Sol-Gel Produced PuO_2 Microsphere Positioned on the Surface of a Sintered UO_2 Pellet Prior to Transient Irradiation. Shrinkage void appears to have formed between the microsphere and the UO_2 matrix.

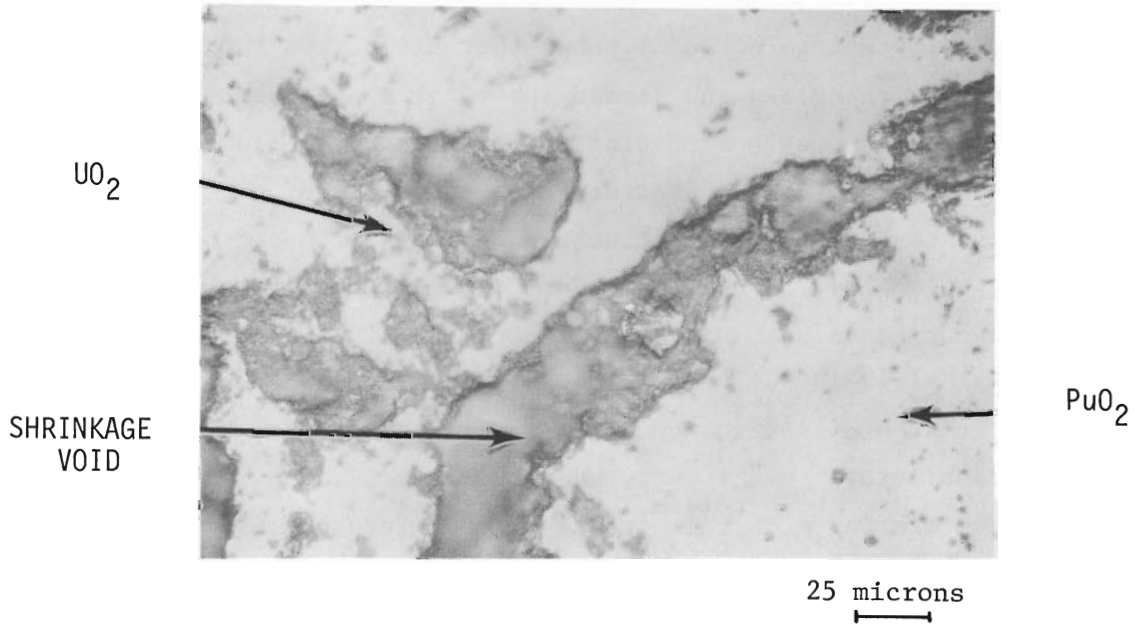

FIGURE 2.3. Shrinkage Void Between a PuO_2 Microsphere and the UO_2 Matrix Prior to Irradiation.

different fuel types.[1,2] The test conditions and results of the transient tests are summarized in Table 2.7.

TABLE 2.7. Summary of Test Conditions and Results of Transient Tests with Pins Containing Discrete PuO_2 Particles in UO_2 Pellet Fuel

Test No.	Energy Deposition, cal/g fuel	Reactor Period, m sec	Maximum Meas. Cladding Temp., °C	Results
1	189	6.78	1450	No visible external effect
2	200	6.22	1600	No visible external effect
3	213	5.79	1725	Two clad penetrations by PuO_2 particles about 600 micron diameters
4	237	5.32	1825	Three clad penetrations 1000 to 1200 micron diameters by PuO_2 particles. Clad severely wrinkled, indicative of incipient melting.

Detailed metallographic examination of the pin irradiated at the lowest energy level (189 cal/gm of fuel) shows that all of the PuO_2 microspheres became molten or vaporized and formed spherical shells about twice their original diameter in the surrounding UO_2 fuel matrix (Figure 2.4). The PuO_2 microspheres have the characteristic appearance of once-molten oxide fuel, i.e., a central subgrain structure region surrounded by a well-defined, high-density, pore-free region. Stain etching techniques delineated what appeared to be a diffusion zone in the outer region of the pore-free band in some PuO_2 particles. A sharp demarcation exists between the PuO_2 microspheres and the UO_2 matrix although changes in the texture of the microstructure in the surrounding UO_2 matrix occurred to a distance of about 1200 microns from the surface of the microspheres. In some cases, the vaporized or molten PuO_2 extruded into pre-existing cracks for distances up to 1000 microns. There was no evidence of PuO_2 in other cracks which formed during cooldown after the transient. PuO_2 microspheres located adjacent to the cladding in the pin irradiated at 189 cal/g of fuel may have caused localized overheating of the cladding into the beta

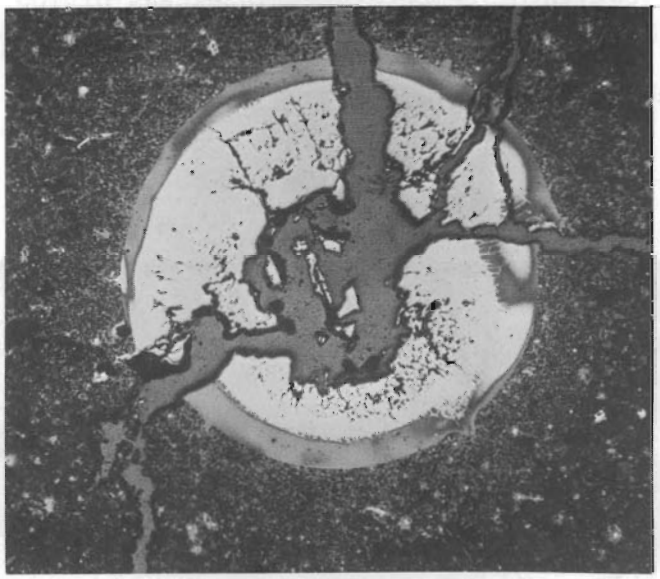

200 microns

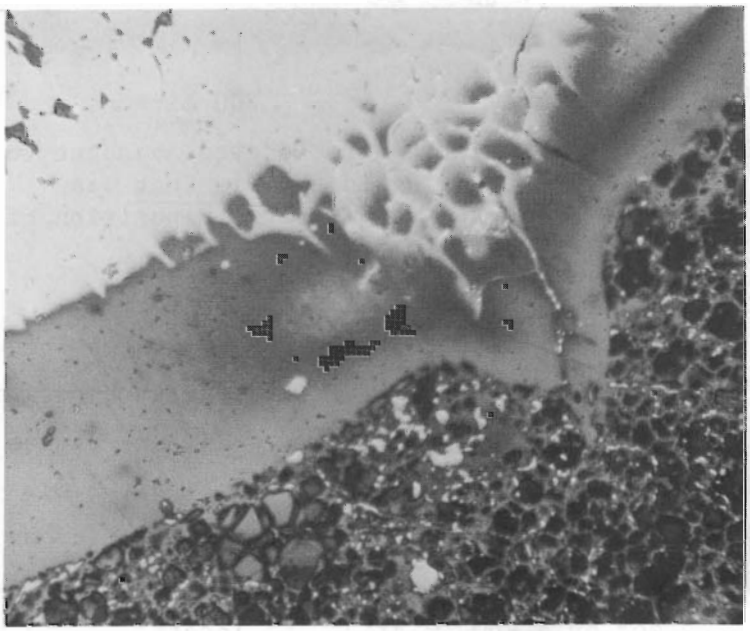

25 microns

FIGURE 2.4. PuO_2 Microsphere Located 2600 Microns from the Surface of the UO_2 Pellet in the Pin that was Subjected to an Energy Deposition of 189 cal/g of Fuel. A diffusion zone formed in the outer part of the pore-free band in the PuO_2 particle.

phase region, indicative of temperatures in excess of 1000°C (Figure 2.5). This localized hot spot resulted in an increased thickness in the zirconium oxide layer on the cladding.

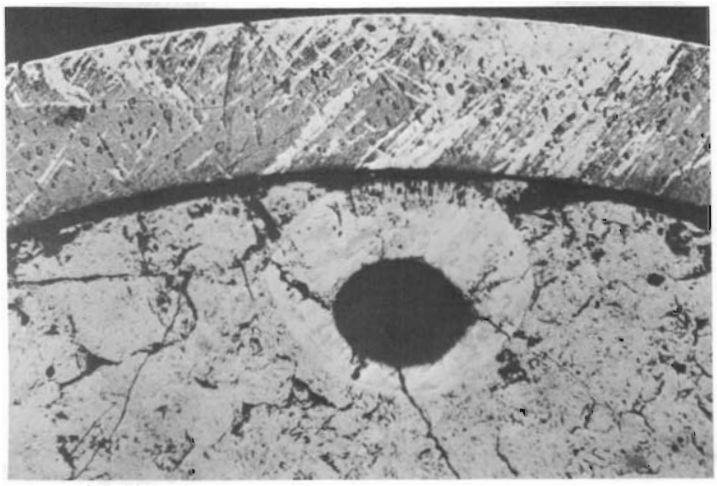

FIGURE 2.5. PuO_2 Microsphere Located Adjacent to the Cladding in the Pin that was Subjected to an Energy Deposition of 189 cal/g of Fuel

Cladding temperatures (~1725°C) near the melting point of Zircaloy-2 were measured in the pin that had a transient energy deposition of 213 cal/gm of fuel. The increased energy deposition resulted in perforation of the cladding by two PuO_2 microspheres (Figure 2.6). Other than the two localized penetrations, which were about 600 microns diameter, the cladding appeared to be relatively unaffected by the irradiation. One penetration was caused by a PuO_2 microsphere located on the surface of a pellet adjacent to the cladding and the other was caused by a PuO_2 microsphere located 100 microns from the surface. It should be noted that not all of the PuO_2 particles located at or near the cladding in this pin

caused penetrations. Cladding penetration occurred by localized melting during the expulsion of the molten or vaporized PuO_2 particle. The cladding area in the vicinity of the penetrations is characterized by the formation of a thick zirconium oxide layer, an oxygen-rich diffusion zone, and beta-transformed structure, all indicative of the high temperatures that existed.

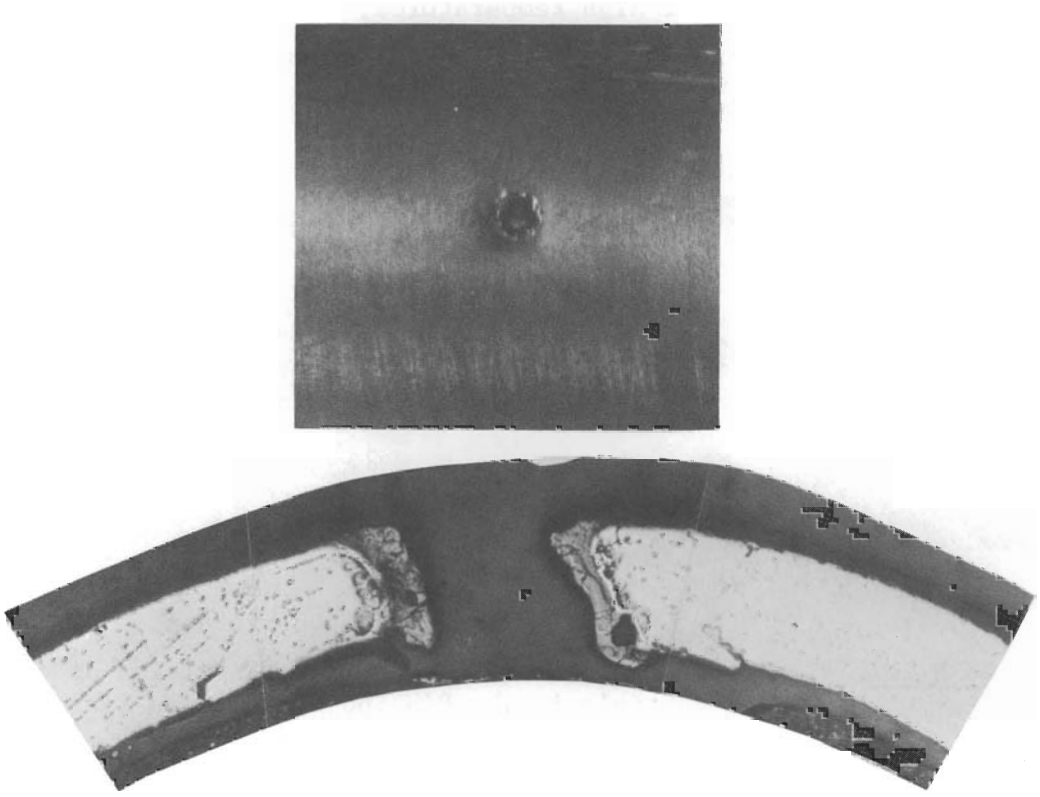

FIGURE 2.6. Cladding Penetration Caused by the Expulsion of a PuO_2 Microsphere in the Pin Subjected to an Energy Deposition of 213 cal/g of Fuel.

Severe cladding wrinkling and deformation indicative of an incipient melting condition occurred in the pin subjected to an energy deposition of 237 cal/gm of fuel. This behavior is characteristic of pins which do not contain abnormally large PuO_2 microspheres tested at these energy levels. In addition to cladding failure by general melting, three localized penetrations were caused by the expulsion of PuO_2 microspheres (Figure 2.7).

The three PuO_2 microspheres which caused cladding penetrations ranging from 1000 to 1200 microns diameter were located at the surface, 100 microns and 800 microns from the surface of pellets in the pin. Again, not all of the PuO_2 particles located at or near the cladding in this pin caused penetrations, even though the cladding was molten sometime during the test (Figure 2.8). A thick zirconium oxide layer and an oxygen-rich diffusion zone, which are indicative of high temperatures, were generally present on the surface of the cladding and were contiguous around the circumference of the cladding penetration (Figure 2.7).

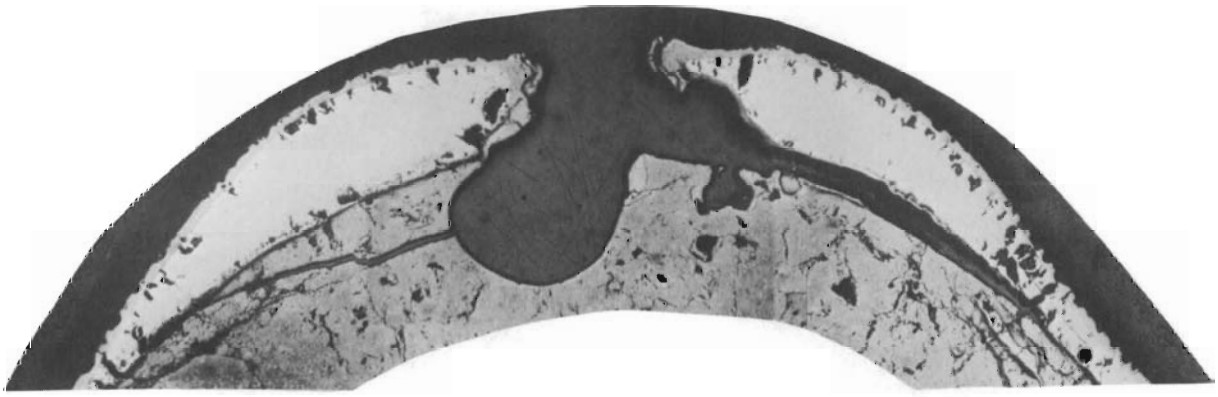

FIGURE 2.7. Cladding Penetration Caused by the Expulsion of a PuO_2 Particle in the Pin Subjected to an Energy Deposition of 237 cal/gm of Fuel (Cladding Temperature was Above Melting Sometime During the Transient Irradiation.)

An electron microprobe analysis conducted on a PuO_2 particle contained in the pin subjected to an energy deposition of 213/cal/gm of fuel indicates that significant uranium dissolution and/or diffusion occurred during the transient (Figure 2.9). The particle, which increased to a diameter of over 1100 microns as a result of the short duration power burst, was scanned radially with a 1 micron diameter beam in 5 micron intervals. The results show that a maximum PuO_2 concentration of about 13 percent occurs at the edge of the center void in the particles. The PuO_2 concentration decreases to about 8 percent at the edge of the surrounding high density, pore-free region, where the concentration abruptly

increases to a constant value of about 10 percent. An abrupt decrease to a constant value of about 3 percent PuO_2 occurs in the outer region of the pore-free band and then decreases to essentially zero beyond the particle boundary. A stain etching technique reveals the outer area of the pore-free region as a distinct zone. Similar PuO_2 particles in the UO_2 matrix of irradiated pins were easily discernable by neutron radiography.

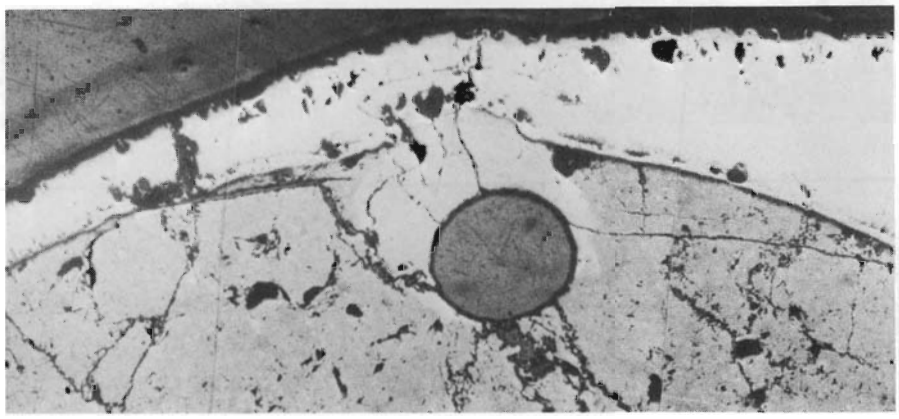

FIGURE 2.8. PuO_2 Microsphere Located Adjacent to the Cladding in the Pin that was Subjected to an Energy Deposition of 237 cal/gm of Fuel. (Penetration did not occur even though the cladding temperature was above melting sometime during the transient.)

These tests demonstrate that below the energy deposition range of 200 to 213 cal/gm of fuel, the energy generated in a single 550 micron diameter PuO_2 microsphere is readily absorbed by the surrounding UO_2 matrix and no external effects occur. Above this energy range, large PuO_2 particles near the surface (0 to 800 microns) of oxide pellets can penetrate the cladding. The ability of a PuO_2 particle to penetrate the cladding depends on the direction that the molten or vaporized particle is accelerated, because not all particles at or near the surface caused cladding penetration. It appears that cladding penetration does not occur if the impinging particles are driven or deflected in a direction that is not normal to the cladding surface. Local cracks that weaken the surrounding matrix also influence cladding perforation.

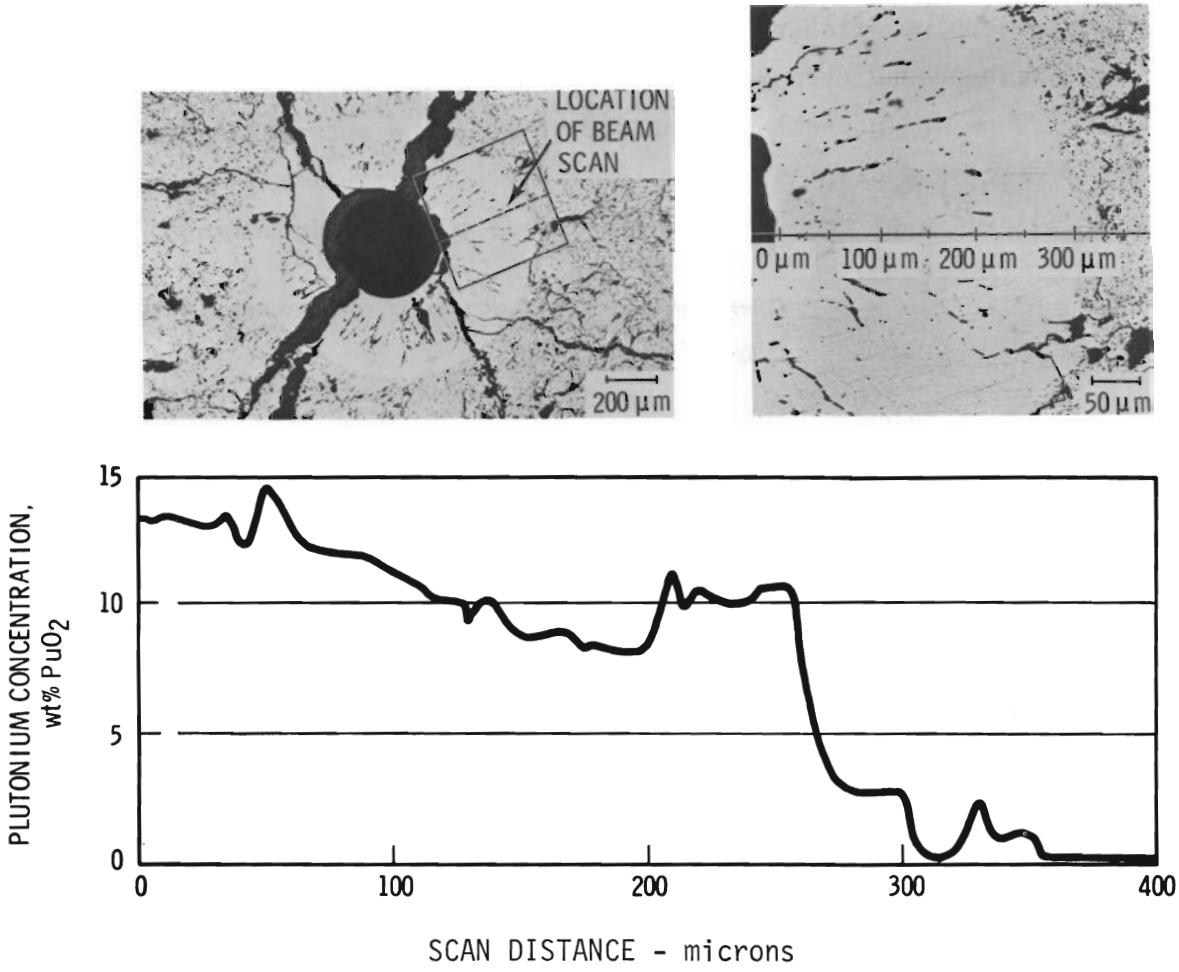

FIGURE 2.9. Radial Plutonium Concentration in a PuO_2 Particle After Irradiation in the Pin Subjected to an Energy Deposition of 213 cal/gm of Fuel Indicates that Considerable Uranium Dissolution Occurred. Electron Microprobe Analysis was made with a 1 Micron Diameter Beam Using 5 Micron Intervals.

The results of these tests show that the effect of the large PuO_2 particles was to slightly reduce the cladding failure threshold energy from the range of 225 to 274 cal/gm of fuel to the range of 200 to 213 cal/gm of fuel. There were no indications of the effects of prompt fuel dispersal caused by the expulsion of the PuO_2 particles into the surrounding water when tested at these energy levels.

Because the presence of single 550 micron diameter PuO_2 particles in mixed-oxide fuels does not appear to significantly effect the cladding

failure threshold energy from that of mixed-oxide fuels with the normal PuO_2 particle size distribution, product specifications which limit the maximum PuO_2 particle size below 550 microns diameter do not appear to be warranted from the standpoint of transient fuel performance considerations. Specifications should be developed which limit the maximum PuO_2 particle size. These experiments have shown that such a limit is greater than 550 microns diameter.

References

1. *W. G. Lussie, "The Response of UO_2 Fuel Rods to Power Bursts: Detailed Tests on 5/16-inch OD, Pellet Fuel, Zircaloy Clad Rods," IN-ITR-112, January 1970.*

2. *W. G. Lussie, "The Response of Mixed-Oxide Fuel Rods to Power Bursts," IN-ITR-114, April 1970.*

3. HIGH TEMPERATURE REACTOR PHYSICS PROGRAM

DERIVATION OF CORRECTIONS TO k_∞ IN THE TWO-GROUP APPROXIMATION

E. P. Lippincott

A report has been prepared which contains some rederivations of corrections to k_∞ for both the poisoned and unpoisoned techniques. The derivations are carried out in the two energy-group approximation. The multigroup definition of k_∞ is used, which reduces to

$$k_\infty = \frac{\text{neutrons produced}}{\text{neutrons absorbed}} = \frac{\nu_1\Sigma_1^f\phi_1 + \nu_2\Sigma_2^f\phi_2}{\Sigma_1^a\phi_1 + \Sigma_2^a\phi_2} \tag{1}$$

in the two-group approximation. In this expression, 1 refers to the epithermal neutron group and 2 to the thermal group.

The formula for the mismatch correction to k_∞ in the unpoisoned technique was originally presented by Heineman.[1] Errors in sign were suspected in this formulation and so the mismatch correction has been rederived, using the same formalism that was used in a previous paper on the definition of k_∞ and the derivation of the two-group expression for the unpoisoned technique without mismatch.[2]

The expression for k_∞ including mismatch may be written as:

$$\begin{aligned} k_\infty = 1 &- \left(\frac{\Delta\rho^{\text{cell}}}{\Delta\rho^{p}}\right)\frac{\left(\Sigma_2^{p}V_p\phi_2^{p'}\right)}{\left(\Sigma_2^{a}V\phi_2'\right)_{\text{cell}}}\left(1 + \frac{\phi_1^+}{\phi_2^+}\frac{\Sigma_1^{p}\phi_1^{p'}}{\Sigma_2^{p}\phi_2^{p}}\right) \\ &- \frac{\left(1+\tau B^2\right)\left(1+L^2B^2\right)\left(1-p\right)L^2B^2}{1+\left(1-p\right)L^2B^2} + \frac{\tau B^2\left(1+L^2B^2\right)\left[\tau B^2 - \eta_1 f_1\left(1-p\right)\right]}{1+\tau B^2 - \eta_1 f_1\left(1-p\right)} \\ &- \frac{\tau B^2\left(1+L^2B^2\right)}{1+\tau B^2-\eta_1 f_1\left(1-p\right)}\left(\frac{\Delta\Phi}{\Phi} + \frac{\Delta\Phi^+}{\Phi^+}\right) + \frac{\left(1+L^2B^2\right)\left(1-\eta_1 f_1\left(1-p\right)\right)}{1+\tau B^2-\eta_1 f_1\left(1-p\right)} \\ &\frac{\Delta\Phi}{\Phi}\frac{\Delta\Phi^+}{\Phi^+} \end{aligned} \tag{2}$$

where now $\Delta\rho^{cell}$ and $\Delta\rho^{p}$ are measured in the mismatched spectrum. If epithermal fissions are neglected, this expression agrees with Heineman's[1] except for the sign of the $\Delta\Phi^{+}/\Phi^{+}$ term. The mismatch correction is seen to reduce to the poisoned technique expression[3,4] when $B^2 = 0$.

If epithermal copper absorptions are small, the difference between Equation 2 and a similarly formulated poisoned technique expression is given by:

$$\delta = \frac{\left(\tau B^2\right)2\left(1 + L^2B^2\right)}{1 + \tau B^2 - \eta_1 f_1\left(1 - p\right)}\left[1 - \eta_1 f_1\left(1 - p\right)\right]^{-1} \tag{3}$$

If the epithermal fissions are neglected, this term reduces to the correction term as derived by Heineman.[1]

An improvement to Equation 2 may be made by eliminating the buckling, which cannot be calculated to the accuracy of the experimental measurement. Solving for B^2 to second order,

$$B^2 = \frac{1}{\tau + pL^2}\left(k_\infty - 1\right) - \frac{pL^2\left[\tau - L^2\left(1 - p\right)\right]}{\left(\tau + pL^2\right)^3}\left(k_\infty - 1\right)^2 \tag{4}$$

$$k_\infty - 1 = \frac{A}{1 + \dfrac{a_1}{\tau + pL^2}} - A^2\frac{\left\{a_2\left(\tau + pL^2\right) - a_1 pL^2\left[\tau - L^2\left(1 - p\right)\right]\right\}}{\left(\tau + pL^2 + a_1\right)^3} \tag{5}$$

where

$$A = \left(-\frac{\Delta\rho^{cell}}{\Delta\rho^{p}}\right)\frac{\left(\Sigma_2^p\phi_2 V\right)^p}{\left(\Sigma_2\phi_2 V\right)^{cell}}\left(1 + \frac{\phi_1^{+\prime}}{\phi_2^{+\prime}}\frac{\Sigma_1^p\phi_1^{p\prime}}{\Sigma_2^p\phi_2^{p\prime}}\right) + \frac{\Delta\Phi}{\Phi}\frac{\Delta\Phi^{+}}{\Phi^{+}} \tag{6}$$

$$a_1 = L^2\left(1 - p\right) + \frac{\tau\eta_1 f_1\left(1 - p\right)}{1 - \eta_1 f_1\left(1 - p\right)} + \frac{\tau}{1 - \eta_1 f_1\left(1 - p\right)}\left(\frac{\Delta\Phi}{\Phi} + \frac{\Delta\Phi^{+}}{\Phi^{+}}\right) - \frac{L^2\left[1 - \eta_1 f_1\left(1 - p\right)\right] - \tau}{1 - \eta_1 f_1\left(1 - p\right)}\frac{\Delta\Phi}{\Phi}\frac{\Phi^{+}}{\Phi^{+}} \tag{7}$$

and

$$a_2 = \left(1 - p\right)L^2\left(\tau + pL^2\right) - \frac{\tau}{1 - \eta_1 f_1\left(1 - p\right)}\left[\frac{\tau}{1 - \eta_1 f_1\left(1 - p\right)} - L^2\eta_1 f_1\left(1 - p\right)\right] + \frac{\tau L^2\left[1 - \eta_1 f_1\left(1 - p\right)\right] - \tau^2}{\left[1 - \eta_1 f_1\left(1 - p\right)\right]^2}\left(\frac{\Delta\Phi}{\Phi} + \frac{\Delta\Phi^+}{\Phi^+} + \frac{\Delta\Phi}{\Phi}\frac{\Delta\Phi^+}{\Phi^+}\right) \quad (8)$$

The evaluation of k_∞ using Equation 5 results in the two-group experimental value least dependent on theoretical calculation.

References

1. *R. E. Heineman, "On the Interpretation of Reactivity Measurements of Reactor Media," Proc. ANS., vol. 8, no. 2, p. 532 (1965).*

2. *E. P. Lippincott, C. R. Richey, D. D. Lanning, "Definition of the Infinite Neutron Multiplication Factors Measured by the PCTR Poisoned and Unpoisoned Technique," Reactor Physics Quarterly Report, July, August, September 1969, BNWL-1240. Battelle-Northwest, Richland, Washington.*

3. *D. J. Donahue, D. D. Lanning, R. A. Bennett, and R. E. Heineman, "Determination of k_∞ from Critical Experiments with the PCTR," Nucl. Sci. Eng., vol. 4, p. 297 (1958).*

4. *D. D. Lanning, "On the Theory of PCTR Experiments," Reactor Physics Quarterly Report, January, February, March 1969, BNWL-1053. Battelle-Northwest, Richland, Washington.*

IMPROVED EXPERIMENTAL CAPABILITY AT HTLTR

R. G. Clark

Modifications were recently made to the safety circuit at HTLTR to reduce the number of unscheduled scrams, reducing the number of times the four reactor safety blades were thermally cycled. Recent operating experience had indicated that the service life of these components varied directly as the number of thermal cycles that they were exposed to at temperatures above 600°C. Changing the safety circuit logic to require two simultaneous off-normal events to trip the circuit instead of one has reduced significantly the number of unscheduled shutdowns. It is expected that this modification will prolong the life of the safety blades.

Additional benefit has also resulted from this change. The unexpected thermal stability of the reactor, that now occurs during experimental runs in which unscheduled scrams have been essentially eliminated, has increased the resolution of the experimental data by almost an order of magnitude over that obtained on the first two experiments.

DEFORMATION IN THE VERTICAL SAFETY RODS AT THE HIGH TEMPERATURE LATTICE TEST REACTOR

R. G. Clark

Since the modification to the blades of the four Vertical Safety Rod (VSR) assemblies was completed in August 1970, one experimental run at temperatures through 1000°C has been completed. The service and exposure given to the safety blades is summarized in Table 3.1. Here one cycle means a full insertion and withdrawal of a VSR blade.

TABLE 3.1. Number of VSR Cycles

	Temperature °C				
VSR	300	550	700	1000	Total
1	60	44	20	17	141
2	44	52	20	18	134
3	42	51	20	17	130
4	44	52	20	18	134
Hours system at temperature	480	312	312	348	1452

Two poison plates in each VSR assembly were filmed at room temperature prior to operation, after the run at 550°C, and every 20 cycles thereafter. As it turned out, they were filmed twice after 550°C, immediately after the 700°C run and then after the 1000°C run.

Each film negative was examined immediately. The results, after comparing 32 film negatives for two poison plates for every VSR, are briefly:

- The predicted deformation has started.

- The amount of deformation and the rate of deforming of the poison plates is significantly less than that which occurred prior to their modification.
- The maximum amount of deformation that has been observed is 44 mils. Deformation of 330 mils is judged necessary to prevent the movement of a VSR blade.
- Small but observable deformation started during operations through 550°C. The threshold temperature for deformation to begin had been predicted to be 550°C to 600°C, with observable deformation occurring at higher temperatures.
- The deformation measured on almost all poison plates after 1000°C was less than that measured after 700°C. Apparently an annealing effect has occurred. For example, the point of maximum deformation for any plate after 700°C was 44 mils as above, and at that same point on the same plate after exposure and cycling at 1000°C, 34 mils was observed. In many instances, the reduction in deformation was greater than this, and in no instance was the resulting deformation on any plate after operation at 1000°C greater than it was at 700°C.
- From a careful examination of the films and, as before, assuming that the deformation of the poison plates as seen on the films is representative of all poison plates in the VSR's, the plastic deformation due to temperature cycling is not expected to limit operation at full design temperature for the scheduled experiments yet to be completed in the facility; namely, the Molten Salt Experiment now under way and the Plutonium Oxide Experiment, scheduled to follow.

MEASUREMENT OF k_∞ FOR A ThO_2 - $^{235}UC_2$ HTGR LATTICE AS A FUNCTION OF TEMPERATURE

T. J. Oakes

Final values of k_∞ have been obtained for the first full temperature range HTGR experiment[1,2] in the HTLTR. The results have been revised from values previously reported due to a re-evaluation of the room

temperature foil activation data and reactivity correction terms. The revised values are listed in Table 3.2.

TABLE 3.2. k_∞ for a ThO_2 - $^{235}UC_2$ Lattice

Temperature °C	k_∞ (Measured)
20	1.111 ± 0.013
150	1.096 ± 0.013
300	1.081 ± 0.013
550	1.055 ± 0.014
700	1.037 ± 0.015
1000	1.032 ± 0.013

References

1. *T. J. Oakes and C. R. Richey, Reactor Physics Quarterly Report, April, May, June 1970, BNWL-1381-2. Battelle-Northwest, Richland, Washington, (August 1970).*

2. *T. J. Oakes, Technical Activities Quarterly Report, July, August, September 1970, BNWL-1511-1. Battelle-Northwest, Richland, Washington, (October 1970).*

MEASUREMENT OF k_∞ FOR A ThO_2 - $(^{233}U,Th)O_2$ - C HTGR LATTICE AS A FUNCTION OF TEMPERATURE

T. J. Oakes

The experimental program to determine $k_\infty(T)$ for the third lattice in a series of measurements in support of the High Temperature Gas-Cooled Reactor (HTGR) program has been initiated. Foil irradiations and reactivity measurements at room temperature have been completed. Measurements of reactivity worths of sample blocks have been completed at temperatures of 150°C, 300°C, and 555°C.

The test lattice consists of a ThO_2 - $(^{233}U,Th)O_2$ - C fuel mixture contained in graphite blocks. Each block consists of a 3-3/4 × 3-3/4 × 24-inch block of graphite containing twenty-five 0.470-inch diameter fuel channels in a 5 × 5 array of 3/4-inch pitch. The fuel channels are

filled with a mixture of graphite powder, ThO_2 powder, and pyrolytic carbon-coated ThO_2 - $^{233}UO_2$ particles. The ThO_2 - $^{233}UO_2$ particles have a kernel diameter of ∿320 μ and a coating thickness of ∿100 μ. The Th/^{233}U ratio in the particles is 3/1. The as-loaded atom ratios for the material being investigated are: C/Th ∿ 278, C/^{233}U ∿ 13756.

The infinite medium neutron multiplication factors for this third HTGR array, listed in Table 3.3, have been calculated via the two-group formulation:[1]

$$k_\infty' = \frac{\nu_1\Sigma_1^f\phi_1 + \nu_2\Sigma_2^f\phi_2}{\Sigma_1^a\phi_1 + \Sigma_1^a\phi_2}$$

The two-group fluxes, ϕ_1 and ϕ_2, were generated from a fundamental mode calculation using HFN.[2] The two-group constants were generated using GRANIT[3] and EGGNIT.[4] The results show that a relatively small total change of 32×10^{-3} in k_∞ is to be expected over the temperature range from room temperature to 1000°C.

TABLE 3.3. Calculated $k_\infty'(T)$ for a ThO_2 - $^{233}UO_2$ Lattice

Temperature °C	k_∞ (Calculated)
20	1.101
150	1.0904
300	1.0824
555	1.0746
700	1.0719
1000	1.0686

References

1. *T. J. Oakes and C. R. Richey, Reactor Physics Department Quarterly Report, April, May, June 1970, BNWL-1381-2, Battelle-Northwest, Richland, Washington, (August 1970).*
2. *J. R. Lilley, "Computer Code HFN - Multigroup, Multiregion Neutron Diffusion Theory in One Space Dimension," HW-71545, Hanford Laboratories, November, 1968.*
3. *C. L. Bennett, "GRANIT: A Code for Calculating Position Dependent Thermal Neutron Spectra in Doubly Heterogeneous Systems by the Integral Transport Method," BNWL-1522-1. Battelle-Northwest, Richland, Washington, (October 1970).*

4. *C. R. Richey, "EGGNIT: A Multigroup Cross Section Code," BNWL-1203, Battelle-Northwest, Richland, Washington, (November 1969).*

DESIGN OF MSBR EXPERIMENT IN THE HTLTR

E. C. Davis and E. P. Lippincott

A reactor lattice physics experiment is currently being designed for the High Temperature Lattice Test Reactor (HTLTR) in support of the Molten Salt Breeder Reactor (MSBR) program. The lattice to be measured will utilize solid fuel in lieu of actual molten salt fuel. The dimensions of the fuel channels and the composition of the fuel mixture are designed to provide physics parameters close to those of the MSBR design.

The standard lattice is being constructed of graphite blocks 3-3/4 inch square with four fuel channels 0.786-inch in diameter. The fuel channels are filled with a mixture of graphite particles, ThO_2 particles and $^{233}UO_2$ - ThO_2 pyrocarbon-coated microspheres. The mixing of the fuel blend and loading into the blocks is carried out with similar materials and methods as were used in loading the blocks for the HTGR lattices previously measured in the HTLTR. At present, 45% of the fuel blocks, exclusive of the central cells, have been loaded. The completed blocks have a $C/^{233}U$ atom ratio of about 9700 and C/Th ratio of about 150.

The central cells to be used in the MSBR experiment are shown in Figure 3.1. The results to be obtained from measurements on these cells are listed in Table 3.4. The standard central cell will be used to measure k_∞ for the lattice. Perturbations of the standard central cell design will be used to determine other coefficients necessary to predict the reactor physics behavior of an actual MSBR.

Three cells will be constructed as shown in Figure 3.1a: the standard cell, a cell with V_2O_3 in place of the ThO_2 to determine the thorium resonance integral, and a reduced density cell for the density coefficient. The cells in Figure 3.1b and 3.1f have the same volume of fuel as the standard cell and will provide information on fuel geometry effects. Other effects of geometry with different amounts of fuel will be measured by cells illustrated in Figure 3.1c, d and e, and replacement of these cells

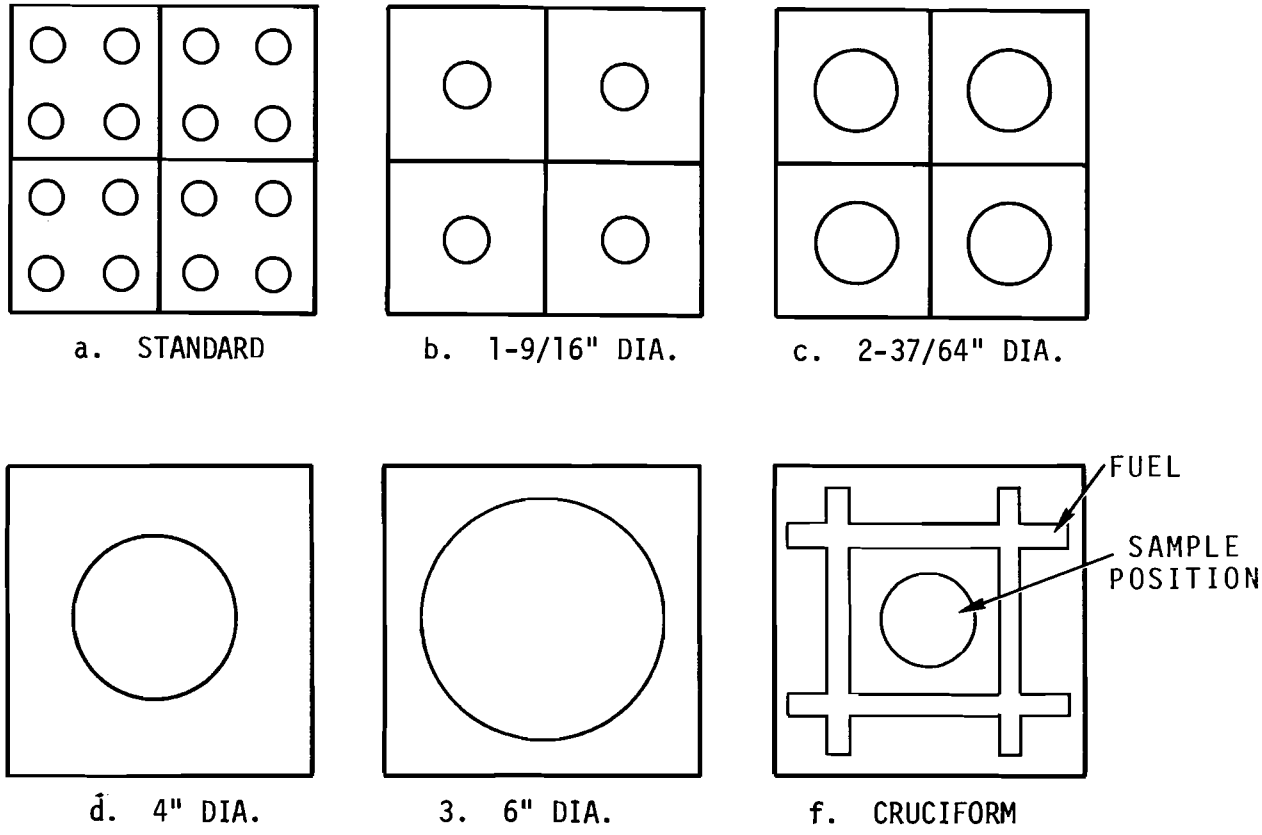

FIGURE 3.1. 7-1/2" × 7-1/2" × 24" Central Cells

with a solid graphite block will indicate graphite control rod worths. A second block, as in Figure 3.1f, will be constructed with Hastelloy N in place of the fuel to measure shutdown rod worth. The sample position in the cruciform block will be used to measure material worths by substitution of the various elements that would be used in an MSBR. The lithium and florine worths will be measured using LiF and teflon.

TABLE 3.4. MSBR Experimental Measurements in HTLTR

Standard Lattice k_∞	
Th Resonance Integral	
Fuel Density Coefficient of Reactivity	
Effects of Fuel Geometry	
Graphite Control Rod Worth	
Shutdown Rod Worth	
Material Worth Measurements	
Copper	^{233}U
Graphite	^{235}U
Beryllium	^{239}Pu
Lithium	INOR-8 (Hastelloy N)
Florine	^{233}U - Th - C Fuel Mixture
Thorium	

Measurements will be made at room temperature, 300°C, 627°C, and 1000°C, except for the teflon (to 300°C only) and the LiF and Be (to 627°C only). The 627°C measurements will provide important data at the MSBR design operating temperature. The 300°C and 1000°C measurements will provide data for evaluation of temperature coefficients at the operating temperature. Measurements between room temperature and 627°C will provide data useful in design of the control system for startup.

Preliminary calculations have been carried out using EGGNIT, GRANIT, and 2-DB to predict k_∞ for the lattice and the estimated mismatch with various loadings in the HTLTR. Final calculations to determine k_∞ for the central cell to compare with the experiment will be carried out after the cell

is loaded and the exact fuel concentration determined. The preliminary calculation gives values for k_∞ of 1.044 at 20°C and 1.001 at 1000°C.

In the 2-DB calculations, MSBR lattice blocks were loaded in a 6 × 6 array (the geometry is identical to the HTGR lattices) and one row of lattice blocks surrounded the array making a total 8 × 8 array. In the HTGR-2 and HTGR-3 experiments, ^{235}U blocks from HTGR-1 were left in this outer row. Using the ^{235}U blocks in this position for the MSBR experiment the mismatch was 0.5% at room temperature and 1.1% at 1000°C. The mismatch is defined by:

$$\text{Mismatch} = \frac{\left(\phi_1/\phi_2\right)_c - \left(\phi_1/\phi_2\right)_e}{\left(\phi_1/\phi_2\right)_c} \quad ,$$

where $\left(\phi_1/\phi_2\right)_c$ is the flux ratio at the radial center of the reactor and $\left(\phi_1/\phi_2\right)_e$ that at the edge of the 6 × 6 MSBR lattice, as calculated by 2-DB. If the ^{235}U blocks are replaced by HTGR-3 blocks or MSBR blocks, the room temperature mismatch becomes 5.4% or 2.2% respectively. In all cases the spectrum was slightly too thermal. These calculations indicate the ^{235}U blocks should be used again in the MSBR experiment and will provide an adequate flux match.

ROOM TEMPERATURE MEASUREMENTS ON A MSBR LATTICE IN THE HTLTR

E. P. Lippincott

The construction of the fuel blocks for the MSBR lattice and loading into the HTLTR has been completed. The design of this lattice has been previously reported.[1] Loading the HTLTR to critical required 268 feet of driver fuel, which compares favorably with the predicted 250 feet.

The flux match was checked using bare and cadmium-covered gold foils and was found to be satisfactory. Foil irradiations with cell in and cell out were used to obtain the relative reaction rates in the fuel cell and in the copper poison. Analysis of this data, together with the reactivity data, will provide a value for k_∞ at room temperature.

Reactivity measurements at room temperature have also been completed. The reactivity measurements of the standard test cell and other test cells are presented in Table 3.5. These measurements were carried out in a nitrogen atmosphere and have not been corrected for the nitrogen in the void.

TABLE 3.5. Test Cell Measurements

Description	Reactivity, ¢*
Standard Central Cell	4.26
Copper (204.2 gm)	-3.53
Graphite Copper Carrier (1124 gm)	0.47
V_2O_3 Cell	23.03
Increased Density Cell	5.73
4 Hole Cell - 1-9/16-inch Diameter	7.82
4 Hole Cell - 2-37/64-inch Diameter	1.60
Single Hole Cell - 4-inch Diameter	9.02
Single Hole Cell - 6-inch Diameter	-1.52
Cruciform Block	5.05
Graphite Block	13.33

* Uncorrected for N_2 in void

Measurements of the worth of hastelloy safety blade material are shown in Table 3.6. As expected, the hastelloy pieces are quite poisonous, and the worth per piece drops substantially as more pieces are added. Inserting a single piece results in a reactivity change of -36.24¢; whereas adding the fourth piece only had an effect of -19.00¢. Because of the size of the reactivities measured, the errors in these numbers are larger than is usual. The numbers in Table 3.6 are accurate to about ±0.2¢, except for the empty block measurement, which is more accurate.

The material worth measurements made by inserting tubes into the center of the cruciform block are presented in Table 3.7. Each of these

measurements is relative to the solid graphite tube. Results from the measurements on Samples 2 and 3 indicate that the worth/gram of graphite in this region is linear with the value 0.407¢/kg. This value may be used to correct for graphite differences in the other samples. This linearity also indicates that the graphite particles have a negligible corss section difference per gram from the solid graphite.

TABLE 3.6. Hastelloy Block Measurements

Empty Hastelloy Block	12.59¢
Block + one Hastelloy Piece	-23.65¢
Block + two Hastelloy Pieces	
Opposite Positions	-53.67¢
Adjacent Positions	-52.08¢
Block + three Hastelloy Pieces	-75.84¢
Block + four Hastelloy Pieces	-94.84¢

TABLE 3.7. Material Worth Measurements

Sample #	Material	Gm. of Material	Gm. of Graphite	Reactivity, ¢
1	Solid Graphite	-	3764.1	0 (standard)
2	Graphite Powder	-	3054.1	-0.29
3	Void	-	1919.5	-0.75
4	Copper Foil	197.1	1881.6	-3.53
5	Beryllium Rod	2011.6	1847.6	+0.96
6	Teflon Rod (CF_2)	2117.6	1875.3	-0.59
7	^{7}LiF	1311.4	2920.3	-2.04
8	ThO_2	250.0	3044.0	-3.80
9	^{233}U: UO_2 (97.5% $^{233}UO_2$)	8.75	3134.9	+4.72
	ThO_2	25.0		
10	^{235}U: U (93% ^{233}U)	11.36	3110.2	+4.36
11	^{239}Pu: PuO_2 (98% ^{239}Pu)	5.32	3164.1	+4.04
	ZrO_2	70.36		
12	Hastelloy Foil	186.4	1843.7	-3.83
13	Fuel Mix:			
	$^{233}UO_2$ (97.5% $^{233}UO_2$)	30.78	2763.7	-1.75
	ThO_2	1941.8		

All of the reactivities in Table 3.7 are approximately as predicted[2] (relative to copper) except for the fuel mix. The difference in this case is attributible to the difficulty in obtaining an accurate value in this complex geometry when the positive reactivity contribution (^{233}U and graphite) and negative contribution (^{233}Th) so nearly cancel.

References

1. *E. C. Davis and E. P. Lippincott, "Design of MSBR Experiment in the HTLTR," Technical Activities Quarterly Report, AEC Reactor Development and Technology Programs, BNWL-1522-2, Battelle-Northwest, Richland, Washington, (June 1971).*

2. *E. P. Lippincott and E. C. Davis, "Pre-experiment Analysis for MSBR-1 Experiment," to be published.*

A ThO_2-PuO_2 HTGR EXPERIMENT IN HTLTR

D. F. Newman

The fourth High Temperature Gas-Cooled Reactor (HTGR) experiment performed in the High Temperature Lattice Reactor (HTLTR) will use a fuel blend consisting of PuO_2 microspheres, ThO_2 powder, and graphite powder. The kernels of the microspheres are nominally 200 micron diameter PuO_2, >96% theoretical density, fabricated from high exposure plutonium.[1] Each PuO_2 kernel is coated with ∿100 micron-thick pyrolytic carbon, 1.8 gm/cm^3 density. The C/Pu atom ratio for the microspheres is 25. Seven shipments of these microspheres, containing a total of 2.8 kg Pu, have been received from ORNL. Each container of microspheres was opened and checked for surface contamination. Surfaces of all coated microspheres were free from plutonium contamination. A 37 gram sample of the coated microspheres was loaded into a graphite holder and inserted in an oven maintained at 1000°C. This pre-experiment test of heated plutonium microspheres will continue during the month of April to verify the integrity of the microspheres under temperature conditions present in the HTLTR.

Experiment planning, preparation of materials for fuel loading, and pre-experiment analysis were begun for the ThO_2 - PuO_2 HTGR experiment. The ThO_2 required for this fuel loading (150 pounds) is on hand. The fine ThO_2 particles (-65 mesh) were screened out from a large batch of mixed

ThO_2 particles and set aside for this experiment. Approximately 350 pounds of graphite powder will also be required for the fuel mixture. Approximately 100 HTGR blocks, presently containing a ThO_2 - $^{233}UO_2$ fuel mixture, will be emptied and reloaded with the ThO_2 - PuO_2 fuel mixture. The fuel unloading operation was begun during the month of March. Each block is 3-3/4-inch by 3-3/4-inch by 24-inches long. The basic block is carbon (graphite) with 25 longitudinal holes. The holes are 0.47-inches diameter, and are arranged in a square 5 by 5 lattice, with 0.75-inch center-to-center spacing between holes. Each hole is to be packed with a 23-inch length column (0.5-inch graphite caps on each end) of 1,535 grams graphite powder, 657 grams ThO_2 powder, and 44.2 grams of microspheres (a nominal 19.86 grams Pu per loaded fuel block). Over the 23-inch length of the fuel column (excluding the 1-inch length endcap region) the C/Pu atom ratio is 7500 with a C/Th atom ratio of 250. For the 23-inch length section of the loaded fuel blocks, a fundamental mode computer calculation[2] using programs EGGNIT and GRANIT gives $k_\infty = 1.13$ at room temperature. Calculations predict a 70 mk loss in reactivity due to an increase in temperature of 1000°C. Values for k_∞ in the range of 1.1 can be determined accurately, because quantities measured in the HTLTR are proportional to $k_\infty - 1$ of the experimental lattice. This experiment should provide a satisfactory check on the calculational methods used in predicting the effect of plutonium loadings in an HTGR system.

References

1. *R. I. Smith, "ThO_2-PuO_2 HTGR Experiment in HTLTR," BNWL-1522-1, p. 3.3. Battelle-Northwest, Richland, Washington, (October 1970).*

2. *C. R. Richey, Personal Communication, November 1970.*

STATUS OF ENDF/B CROSS SECTIONS FOR HTLTR STUDIES

C. L. Bennett

A thermal cross-section data tape has been derived from ENDF/B-II data for the following isotopes: natural copper, ^{63}Cu, ^{65}Cu, ^{232}Th,

^{233}U, ^{234}U, ^{235}U, ^{236}U, ^{238}U, ^{239}Pu, ^{240}Pu, ^{241}Pu, ^{242}Pu, water, graphite, ^{14}N, and ^{16}O. The data tape has been prepared in the format required by computer code GRANIT.[1] There are two sets of water data both at 296°K. One set has had the diagonals of the scattering kernel corrected for the anisotropic scattering; the other set has both the zeroth and the first moment kernels without correction. Similarly, there are also two sets for the graphite data for each of the following temperatures: 296°K, 400°K, 600°K, 800°K, 1000°K, and 1200°K. The library data for both nitrogen and oxygen also represent these same temperatures. However, Brown-St. John scattering kernels were generated for nitrogen and oxygen. For nitrogen the total scattering cross section from the ENDF/B files was used to obtain least-square-fitted Brown-St. John parameters.

Epithermal cross-section data has been generated via ETOG[2] for the following isotopes: ^{12}C, molybdenum, niobioum, nickel, iron, chromium, ^{235}U, ^{238}U, ^{233}U, ^{232}Th, ^{239}Pu, ^{240}Pu, and ^{241}Pu. The data was processed in GAM-I format. The remaining step is to produce an EGGNIT[3] library tape from this processed data.

These data libraries will be used to assess the effect of ENDF/B-II data on HTLTR calculational results.

References

1. *C. L. Bennett, "GRANIT: A Code for Calculating Position Dependent Thermal Neutron Spectra in Doubly Heterogeneous Systems by the Integral Transport Method," Technical Activities Quarterly Report AEC Reactor Development and Technology Programs, July, August, September 1970, BNWL-1522-1, Battelle-Northwest, Richland, Washington, (October 1970).*

2. *D. E. Kusner, S. Kellman, R. A. Dannels, ETOG-1, A FORTRAN IV Program to Process Data from the ENDF/B File to the MUFT, GAM and ANISN Formats, WCAP-3845-1, Westinghouse Electric Corp., Pittsburgh, Pennsylvania, (December 1969).*

3. *C. R. Richey, EGGNIT: A Multigroup Cross-Section Code, BNWL-1203, Battelle-Northwest, Richland, Washington, (November 1969).*

REVIEW OF THE ENDF/B DESCRIPTION OF CARBON

B. R. Leonard

The neutron scattering cross section of carbon below 2 MeV is classed as a secondary standard against which other scattering cross sections are measured. The status of this cross section was reviewed as part of the efforts of the Normalization and Standards Subcommittee of the Cross Section Evaluation Working Group (CSEWG). The results of this review indicated that the experimental data determined the cross section to within the accuracy requested as a standard. Review of the Versions I and II descriptions of ENDF/B, however, showed that neither version described the cross section adequately. A detailed manuscript of this review was submitted to CSEWG.

4. PHOENIX STUDIES

EVALUATION OF CALCULATIONAL METHODS USED FOR THE PHOENIX BURNUP EXPERIMENT

U. P. Jenquin

The measured lifetime of the Phoenix burnup experiment is substantially shorter than the predicted lifetime.[1] The discrepancy is due primarily to the difference between the measured and calculated burnup slope, with the measured burnup slope being 80 percent larger than the calculated burnup slope. A brief investigation[1] into the calculated burnup slope indicated that the fission product calculation was the prime suspect. The fission products were represented by a pseudo fission product model.

An attempt was made to calculate unsaturated fission product absorptions more accurately by including all the important fission products in ALCHEMY[2] calculations. In these calculations the neutron flux, the macroscopic fission cross section, and the microscopic fission product cross sections are constant throughout burnup. These assumptions have not been evaluated but are estimated not to introduce any major errors in the calculation. The worth of the fission products calculated by ALCHEMY is about the same as the worth calculated by the pseudo fission product model. Therefore, the burnup slope is not changed by a more detailed fission product calculation. Of course the accuracy of the ALCHEMY calculations depends on the accuracy of the individual fission product yields and fission product cross sections. Moreover, most of the neutron absorptions in fission product nuclei occur at energies greater than 0.683 eV, where the fission product cross sections are less accurately known. The calculated burnup slope has an uncertainty of 25 percent due to uncertainties in fission product poisoining. The ALCHEMY calculations indicate that errors in the fission product calculation cannot account for all the discrepancy between the calculated and measured burnup slope. Thus, other aspects of the burnup calculation have been investigated.

A ZODIAC-G[3] burnup calculation was made using the usual ^{240}Pu cross section rather than the wings-240 prescription[1] in HRG3.[4] As

indicated in Reference 1, this change increases the burnup slope by 15 percent, thus accounting for only a small part of the discrepancy. However, this effect also introduces a larger error in the initial reactivity so that the total core lifetime is not changed appreciably.

The transplutonium isotopes were not included in the ZODIAC-G calculation. Based on the number produced from ^{242}Pu captures, the transplutonium isotopes would increase the burnup slope by 5 percent at the most. The production of ^{238}Pu by an (n,2n) reaction with ^{239}Pu has also been ignored in the burnup calculation. This effect is worth less than 1 percent in the burnup slope.

An estimate of the effect of using the "best" available cross-section data for the plutonium isotopes has been made. It is assumed that this data would consist of ENDF/B-II data for ^{239}Pu, ^{240}Pu, and ^{241}Pu. If this data were used, the average capture-to-fission ratio for ^{239}Pu, $\bar{\alpha}^{239}$, would increase about 1 percent. The average microscopic absorption cross section for ^{240}Pu, σ_a^{240}, would increase about 2 percent and $\bar{\alpha}^{241}$ would decrease about 15 percent. Each of these changes is estimated to be worth 1-2 percent at the most in the burnup slope. Using the ENDF/B-II H_2O kernel would increase $\bar{\alpha}^{239}$ by about 1 percent, which in turn would have <1 percent effect on the burnup slope. Another increase in $\bar{\alpha}^{239}$ ($\sim$2 percent) would come about with an increase in the temperature of the water kernel from 20°C to 45°C.

An estimate of spatial burnup effects was made by doing a BRT-I[5] calculation over the 1 eV ^{240}Pu resonance. The results indicate a slight decrease in the burnup slope rather than the expected increase. Although the quantitative results may not be accurate, it is concluded that the effect is sufficiently small that it can be ignored.

The energy obtained from each fission was assumed to be 211 MeV for calculational purposes. Since 5 percent of this energy occurs in the form of neutrinos and is not measured as heat output, the calculated burnup slope should be increased 5 percent when comparing it to the measured

burnup slope. Combining the uncertainties associated with the measured heat output and the reactivity loss, the measured burnup slope probably contains an uncertainty of ±10 percent.

A paper[5] discussing the sensitivity of the burnup slope to microscopic cross-section data has been presented at the Third Conference on Neutron Cross Sections and Technology. Uncertainties in the burnup slope due to uncertainties in the microscopic cross-section data were determined. The results[5] are summarized in Table 4.1.

TABLE 4.1. Sensitivity of the Phoenix Burnup Slope to Microscopic Cross-Section Data[6]

Cross-Section Data	Burnup Slope Uncertainty, %
σ_a^{240}	5
$\bar{\alpha}^{239}$	1
Scattering Kernel for H_2O	0
Thermal Fission Products	4
Nonthermal Fission Products	20

Investigations are continuing in an attempt to understand the discrepancy between the calculated and measured burnup slopes. Isotopic data from the destructive analysis of the irradiated fuel will be used to verify the aspects of the burnup calculation relating to the plutonium isotopes. The fission product calculation will also be looked at more carefully. More emphasis will be placed on the energy range above 0.638 eV. Some of the other estimates mentioned above will also be evaluated more accurately.

References

1. *C. M. Heeb, Analysis of the Phoenix Fuel Experiments, BNWL-1514, Pacific Northwest Laboratory, October 1970.*

2. *B. H. Duane, "Time-Variant Isotopic Transmutation GE-HL Program ALCHEMY", Physics Research Quarterly Report, October, November, December 1963, HW-80020, General Electric Company, January 1964.*

3. *R. H. Holeman and D. D. Matsumoto, ZODIAC-G, A Code for Multigroup, Multiregion Burnup Calculations, BNWL-1559, Pacific Northwest Laboratory, February 1971.*

4. *J. L. Carter, HRG3: A Code for Calculating the Slowing-Down Spectrum in the P_1 or B_1 Approximation, BNWL-1432, Pacific Northwest Laboratory, June 1970.*

5. *C. L. Bennett and W. L. Purcell, BRT-I: Battelle-Revised-THERMOS, BNWL-1434, Pacific Northwest Laboratory, June 1970.*

6. *U. P. Jenquin, Sensitivity of a Plutonium-Fueled Burnup Experiment to Microscopic Cross-Section Data, BNWL-SA-3658, Pacific Northwest Laboratory, March 1971; also to be published in the Proceedings of the Third Conference on Neutron Cross Sections and Technology.*

PHOENIX FUEL STUDIES

J. W. KUTCHER

Postirradiation Analysis of MTR-Phoenix Fuel Plates

The receipt of irradiated fuel plates from the MTR-Phoenix Core occurred during this quarter. A total of 48 plates, from 12 different elements were received from Idaho Nuclear Corporation (INC). The shipments had previously been delayed by INC hot cell problems.

Gamma scanning of these plates is in progress. Full length axial scans are being performed on each plate, followed by a scan across each plate at the position of maximum activity. Gamma spectra will be obtained at selected points.

Upon completion of the gamma scanning, selected plates will be retained for possible destructive analysis to determine plutonium isotopics.

Analysis of Phoenix Flux Wands

The five plutonium flux wands from the MTR-Phoenix Core have been gamma scanned. These wands were located in positions inside fuel elements during the core irradiation. One wand was removed at a core burnup of 225 MWd, a second wand was removed at a core burnup of 660 MWd, while the other three wands were removed at a core burnup of 907 MWd. The gamma scan data show clearly the shift with burnup of the axial position of maximum flux. This shift is due to the withdrawal of the shim rods with burnup.

Six samples from irradiated flux wands and one sample from an unirradiated wand have been destructively analyzed to obtain plutonium isotopic data. The analysis of these data is in progress. These data will provide important correlations with burnup calculations.

Analysis of MTR Experimental Data

Analysis is continuing of data from the MTR-Phoenix experiments. This includes initial startup and zero-power experiments, burnup history, and zero-power experiments at steps during burnup. A final report on the experiment is in preparation.

5. STEADY STATE AND TRANSIENT SUBCHANNEL CODE DEVELOPMENT AND DATA ANALYSIS

D. S. Rowe and B. M. Johnson

The objective of this program is to develop improved methods for analyzing heat transfer and fluid flow in rod bundle nuclear elements during both steady state and transient conditions. The program includes both analytical studies for the continued development of computer programs and experimental studies for the verification and implementation of these computer programs.

COBRA-III COMPUTER PROGRAM

The objective of this portion of the program is to develop a mathematical model and computer program for predicting the steady-state and transient performance of rod bundle nuclear fuel elements.

An interim report is being prepared to describe the present status of the COBRA-III computer program development. Although improvements are continuing, this interim version of COBRA-III will be useful for analysis of many steady state and transient thermal hydraulic problems.

The interim version of the COBRA-III program uses an approach that is very similar to COBRA-II. The bundle flow cross-section is divided into flow subchannels that are assumed to contain one-dimensional flow and are coupled to each other by turbulent and diversion crossflow mixing. Both types of crossflow mixing carry mass, energy and momentum between the subchannels. Boiling and nonboiling conditions are considered by using an equation of state that gives density as a function of enthalpy, flow, heat flux, pressure, position, and time. The model neglects sonic velocity propagation; therefore, it is limited to transients with time duration greater than the time for a sonic wave to pass through the channel. A simplified transverse momentum equation that neglects temporal and spatial acceleration is used to simplify the numerical solution. This gives instantaneous response of the diversion crossflow to changes in subchannel pressure gradient. The equations of the mathematical model are solved by

using a semiexplicit finite difference scheme that is stable for all time steps. This scheme also gives a boundary value flow solution for both steady state and transients, where the boundary conditions are the inlet enthalpy, inlet flow rate and exit pressure. Several successful computer solutions have been run using the above mathematical model and numerical solution. These have included rapid changes in heat flux, inlet flow rate, inlet enthalpy and system pressure. The ability of the boundary value solution to include high crossflow resistance has also been successfully demonstrated. High crossflow resistance has the effect of causing a downstream flow disturbance to be felt upstream. This effect cannot be considered by COBRA-II and other similar computer programs that use an initial value flow solution.

The features of COBRA-III can be summarized as follows:

- It contains all the analysis capability of the COBRA-II program.
- It can consider transients up to, but not including, sonic velocity propagation effects.
- The numerical scheme performs a boundary value solution to more properly include the effects of crossflow resistance.
- The numerical solution is stable for all time steps.

Development of COBRA-III is continuing to improve its capability. Major emphasis is being directed toward developing a more complete transverse momentum equation that includes both spatial and temporal acceleration. This is needed to permit more accurate prediction of subchannel flows in regions where the crossflow is changing rapidly, such as near blockages. A tentative crossflow momentum equation has been developed and incorporated into the COBRA-III program. This equation includes the time rate of change of diversion crossflow and the axial component of transverse spatial acceleration. Although this new equation requires a more complicated finite difference scheme, a stable scheme has been developed and has been successfully tested on sample problems. Evaluation of this more complete mathematical model is continuing. Presently, it appears that the added terms to the transverse momentum equation give greater numerical

stability with little increase in computation time; however, the computer core storage requirements are greater because subchannel data must be stored at two levels of time.

EXPERIMENTAL STUDY OF FLOW STRUCTURE IN ROD BUNDLES

The objective of this experimental study is to obtain a more complete description of the turbulent flow structure of single-phase flow in rod bundles so that better mixing correlations can be developed for use in subchannel computer programs. Present mixing correlations do not adequately account for the effect of subchannel geometry.

This experimental study will investigate the turbulent flow structure in rod bundle geometry to define the effect of subchannel shape, gap spacing and subchannel interconnections. The axial and transverse fluctuating velocity components in the gap and within the subchannels will be the primary measurement in these experiments. Statistical processing of these measurements will permit an estimate of turbulence intensity and scale in rod bundle subchannels. These measurements will be made with a two-component laser-Doppler velocimeter. This device can measure fluid velocities at a point in a flow stream without inserting a probe into the flow. It operates from the principle that light scattered from very small particles moving with the fluid experiences a frequency shift that is related to the fluid velocity. By using a system of optics and electronics, this Doppler shift can be accurately measured to obtain the instantaneous fluid velocity at the measurement point. This measurement technique will enable measurements of velocities that have never been obtained in rod bundle geometries.

Design and fabrication of the experimental apparatus is complete. A common flow channel is being used to accommodate a variety of subchannel sizes and shapes. This is accomplished by using a flow channel that consists of two common side plates containing glass windows for entrance and exit of the laser beam. Inserts of various thicknesses are placed between the side plates to create rectangular flow channels. Subchannels are formed within this channel by inserting rods, or sectors of rods, to form the desired subchannel shapes. Rods with glass windows are being used

where appropriate to enable passage of the laser beam. A flow straightening and calming section is included to control the level of upstream turbulence.

Two types of experiments will be performed. First, turbulence data obtained in a flow channel with a rectangular cross section will be compared with existing hot-wire turbulence data to verify that the laser-Doppler technique produces valid two-component turbulence data. Next, turbulent velocity measurements will be performed in the gap of interconnected subchannels to determine how various subchannel shapes effect the transverse velocity fluctuations that are responsible for mixing. Similar measurements will then be performed in a 9-rod bundle to determine how the turbulent flow structure in multiple connected subchannels differ from the structure in simply connected subchannels. This comparison is expected to help determine the minimum size required for rod bundle turbulent diffusion experiments.

6. PLUTONIUM CRITICALITY STUDIES

CRITICAL EXPERIMENTS WITH UNDERMODERATED MIXTURES OF PuO_2 - UO_2

S. R. Bierman

Associated with the development of Liquid Metal Fast Breeder Reactors will be the need to fabricate, process, and recover large quantities of mixed PuO_2 - UO_2 fuels. Because of the plutonium content, these operations will involve a very large number of potential critical masses. This fuel must be handled in such a manner as to preclude criticality under normal and accident conditions. Criticality considerations will bear heavily on the economics of the entire system. Consequently, it is important that these considerations be based on accurate, reliable data. Also, benchmark type data on clean, homogeneous Pu-U systems in well-defined, simple geometries are needed for testing cross-section data and evaluating computational techniques for calculating geometry and heterogeneity effects.

To provide these needed data, a research effort has been initiated at the Critical Mass Laboratory of Battelle-Northwest. This effort is oriented toward fulfilling Task (8-5.2) - Criticality - of the LMFBR Program Plan. However, attention has also been given to the suggestions of such sources as the Long Range Planning Group at Oak Ridge, Tennessee, especially in the design and planning of less general types of experiments. In the LMFBR Program Plan, emphasis was placed on the need for criticality data on uranium enriched with between 8 and 30 wt% plutonium. Consequently, the initial series of experiments was designed to provide criticality data on hydrogenous mixtures of PuO_2 - UO_2 at concentrations that would provide data over the widest possible range in the 8 to 30 wt% enrichment region.

In the undermoderated region of the neutron spectrum, calculations[1] have indicated that a homogeneous mixture of PuO_2 and UO_2 containing about 30 wt% PuO_2 should exhibit a nearly constant critical volume at atomic H/(Pu + U) ratios below about 50, with the volume possibly being a minimum. The calculations also indicated that a homogeneous mixture of PuO_2 and UO_2 containing about 15 wt% PuO_2 should experience a minimum critical volume at an H/(Pu + U) atomic ratio of about 30. Therefore, experiments with

fuel at 50 and 30 H/(Pu + U) should provide the data needed for establishing the minimum critical volume for PuO_2 - UO_2 systems containing 30 and 15 wt% PuO_2, respectively. This is an important criticality safety parameter, since systems constrained to a smaller volume would be critically safe in all geometries and at all degrees of moderation and reflection.

The calculations also indicated that a mixture of PuO_2 and UO_2 containing 8 wt% PuO_2 would have a minimum critical mass in the undermoderated region of the neutron spectrum at an H/(Pu + U) atomic ratio of about 50. Experiments with fuel at this degree of moderation should provide the data needed for establishing the mass below which criticality is not possible for all 8 wt% enriched PuO_2 - UO_2 systems.

The first two series of experiments have been completed and the third is in progress. The experimental results of the completed measurements are presented in Tables 6.1 and 6.2, and preliminary results from the experiments in progress are presented in Table 6.3.

The first series of measurements was made with PuO_2 - UO_2 - polystyrene compacts having an H/(Pu + U) atomic ratio of 47.4 and a plutonium enrichment of 30 wt%. The second series of measurements was made with compacts having an H/(Pu + U) atomic ratio of 30.6 and a plutonium enrichment of 14.62 wt%. In both sets of fuel, the plutonium contained 8 wt% ^{240}Pu and the uranium was depleted to 0.151 wt% ^{235}U. The particle sizes of the oxides were less than 50 microns, with the average being 10 microns for both sets of fuel.

Experimental data were obtained on both bare and Plexiglas-reflected rectangular parallelepipeds constructed from 2 × 2 × 2-inch fuel compacts. The bare critical assemblies were near-cubic in geometry to permit determining the bare critical cube size for each fuel. The reflected critical assemblies ranged from a near-cubic geometry to thin slabs to permit determining the reflected critical thickness for a slab infinite in two dimensions, in addition to the reflected critical cube size of each fuel. The critical dimensions and masses for each of these critical assemblies are shown in Tables 6.1 and 6.2. The cube and infinite slab values obtained from interpolation and extrapolation of the data are also shown in

TABLE 6.1. Criticality Data for PuO_2 - UO_2 - Polystyrene Fuel Mixtures Containing 30 wt% Pu

Density of Fuel = 373 g (Pu + U)/ℓ; H/Pu + U = 47.4
H/Pu = 158.2; ^{240}Pu Content of Pu = 8.0 wt%; ^{235}U Content of U = 0.151 wt%

Reflector	CRITICAL DIMENSIONS, CM[(a)]			CRITICAL MASS[(a)]	
	Length	Width	Height	kg of Pu	kg of U
Plexiglas	30.54 ± 0.03	30.54 ± 0.03	30.89 ± 0.02	3.23 ± 0.05	7.53 ± 0.12
Plexiglas	35.63 ± 0.04	35.63 ± 0.04	23.95 ± 0.10	3.40 ± 0.05	7.94 ± 0.12
Plexiglas	40.72 ± 0.04	40.72 ± 0.04	20.22 ± 0.05	3.75 ± 0.05	8.76 ± 0.13
Plexiglas	50.90 ± 0.05	45.81 ± 0.05	17.14 ± 0.04	4.48 ± 0.06	10.44 ± 0.16
Plexiglas	61.08 ± 0.06	50.90 ± 0.05	15.62 ± 0.05	5.44 ± 0.08	12.69 ± 0.20
Plexiglas	61.08 ± 0.06	55.99 ± 0.06	15.12 ± 0.02	5.80 ± 0.09	13.51 ± 0.21
Plexiglas	50.90 ± 0.05	50.90 ± 0.05	16.45 ± 0.04	4.78 ± 0.08	11.14 ± 0.18
Plexiglas[(b)]	30.60 ± 0.02	30.60 ± 0.02	30.60 ± 0.02	3.21 ± 0.05	7.49 ± 0.12
Plexiglas[(b)]	∞	∞	10.96 ± 0.04	---	---
Bare	45.81 ± 0.05	40.72 ± 0.04	37.98 ± 0.06	7.93 ± 0.12	18.51 ± 0.78
Bare	40.72 ± 0.04	40.72 ± 0.04	42.24 ± 0.03	7.84 ± 0.11	18.30 ± 0.77
Bare	45.81 ± 0.05	50.90 ± 0.05	32.49 ± 0.02	8.48 ± 0.12	19.80 ± 0.84
Bare[(b)]	41.20 ± 0.05	41.20 ± 0.05	41.20 ± 0.05	7.83 ± 0.11	18.28 ± 0.77

(a) Experimentally determined corrections have been made, accounting for the reactivity effects of the cladding material, the stacking voids, and the structural supports.

(b) Infinite slab thickness obtained by extrapolation of data. Cube dimensions obtained by interpolation between critical assemblies.

TABLE 6.2. Criticality Data for PuO_2 - UO_2 - Polystyrene Fuel Mixtures Containing 14.62 wt% Pu

Density of Fuel = 580 g (Pu + U)/ℓ; H/Pu + U = 30.6
H/Pu = 210.1; ^{240}Pu Content of Pu = 8.0 wt%; ^{235}U Content of U = 0.151 wt%

Reflector	CRITICAL DIMENSIONS, CM[(a)]			CRITICAL MASS[(a)]	
	Length	Width	Height	kg of Pu	kg of U
Plexiglas	30.54 ± 0.03	40.72 ± 0.04	29.81 ± 0.15	3.14 ± 0.04	18.35 ± 0.35
Plexiglas	40.72 ± 0.04	40.72 ± 0.04	23.84 ± 0.10	3.35 ± 0.04	19.57 ± 0.37
Plexiglas	45.81 ± 0.04	50.90 ± 0.05	19.82 ± 0.11	3.92 ± 0.05	22.89 ± 0.44
Plexiglas	50.90 ± 0.05	50.90 ± 0.05	18.92 ± 0.09	4.16 ± 0.05	24.28 ± 0.46
Plexiglas	61.08 ± 0.06	50.90 ± 0.05	17.72 ± 0.09	4.67 ± 0.06	27.28 ± 0.52
Plexiglas	61.08 ± 0.06	61.08 ± 0.06	16.63 ± 0.09	5.26 ± 0.06	30.73 ± 0.59
Plexiglas[(b)]	33.30 ± 0.17	33.30 ± 0.17	33.30 ± 0.17	3.13 ± 0.05	18.28 ± 0.40
Plexiglas[(b)]	∞	∞	11.56 ± 0.09	---	---
Bare	40.72 ± 0.04	40.76 ± 0.17	52.39 ± 0.07	7.37 ± 0.09	43.06 ± 0.82
Bare	40.72 ± 0.04	45.86 ± 0.19	45.10 ± 0.06	7.14 ± 0.08	41.70 ± 0.79
Bare	50.90 ± 0.05	45.86 ± 0.19	36.99 ± 0.05	7.32 ± 0.08	42.75 ± 0.81
Bare[(b)]	43.78 ± 0.07	43.78 ± 0.07	43.78 ± 0.07	7.12 ± 0.08	41.55 ± 0.80

(a) Experimentally determined corrections have been made, accounting for the reactivity effects of the cladding material, the stacking voids, and the structural supports.

(b) Infinite slab thickness obtained by extrapolation of data. Cube dimensions obtained by interpolation between critical assemblies.

Tables 6.1 and 6.2. The values presented in these tables have been experimentally corrected for the reactivity effects of cladding material, stacking voids, and structural supports.

TABLE 6.3. Preliminary Criticality Data for Plexiglas - Reflected PuO_2 - UO_2 - Polystyrene Assemblies[a]

CRITICAL DIMENSIONS,[b]			CRITICAL MASS[c]	
Length	Width	Height	kg Pu	kg U
40.72	45.72	38.73	2.04	23.44
50.90	50.80	31.11	2.28	26.15
61.08	60.96	26.58	2.80	32.17

(a) H/(Pu + U) about 50, and wt% Pu in the Pu + U about 8

(b) Dimensions have not been corrected for cladding and stacking voids

(c) Mass based on blended weights

The critical thickness of a Plexiglas-reflected slab infinite in two dimensions was determined to be 10.96 ± 0.02 cm for the 30 wt% plutonium-enriched-47.4 H/(Pu + U) fuel, and 11.56 ± 0.09 cm for the 14.62 wt% plutonium-enriched-30.6 H/(Pu + U) fuel. The reflected critical cube sizes for each of these fuels were, respectively, 30.60 ± 0.05 cm and 33.30 ± 0.17 cm on a side. The corresponding masses of plutonium were 3.21 ± 0.05 kg and 3.13 ± 0.05 kg, respectively.

The data from these completed experiments can be used for checking cross sections and calculational techniques; however, for general application in establishing criticality safety limits, some theoretical corrections to the data are still needed. A determination of these corrections is in progress.

Reference

1. *L. E. Hansen, S. R. Bierman, R. C. Lloyd and E. D. Clayton, "Criticality of PuO_2 - UO_2 Aqueous Mixtures," Transactions, American Nuclear Society, 12, 869 (1969).*

THE EFFECT OF FIXED AND SOLUBLE NUCLEAR POISONS ON CRITICALITY

R. C. Lloyd and L. E. Hansen

Soluble Gadolinium as Neutron Absorber

The overall objectives of these experiments are to establish the effect of the absorber on criticality, and obtain those data which lead to a workable theory of absorption of such poisons, permitting the handling, storage, shipment, and processing of fissile materials with reduced probability of criticality. A distinct advantage in using soluble poison for criticality prevention in certain applications is that the neutron absorber would remain with the fissile material irrespective of its location. Solution leaking from a vessel into a more reactive geometry would not be cause for concern, so long as the absorber remained in solution.

Criticality experiments were carried out for determining the effect of soluble poisons on the criticality of plutonium nitrate solution. A series of measurements was performed with highly concentrated plutonium solution poisoned with gadolinium. The plutonium concentration was ∿370 g Pu/ℓ (^{240}Pu content of 8.3 wt%). The gadolinium concentration was varied from ∿4 to ∿21 g Gd/ℓ. The experiments utilized a 24-inch diameter, water-reflected, stainless steel cylindrical vessel. Preliminary results indicate the gadolinium to be significantly less effective than expected for the neutron spectrum of the 370 g Pu/ℓ solution. The data from the experiments are under analysis. Preliminary criticality data are given in Table 6.4.

The solution containing ∿13 g Gd/ℓ was permitted to stand for one month. The criticality measurement made after this time period correlated exactly with the previous measurement made with the same solution, which indicates stability of the Gd-poisoned solutions in storage.

The KENO multigroup Monte Carlo code was used to compute criticality factors (k_{eff}) for experimental critical systems initially determined in the first series of experiments. In those experiments, the plutonium concentration of the gadolinium-poisoned solutions was 116 g Pu/ℓ, and the free acid molarity was 1.85. The multigroup cross-section data (18 energy

groups) were obtained by means of the GAMTEC-II code. The gadolinium cross section data were from the ENDF/B-II library. Each of the computed criticality factors (k_{eff}) were based on 10,000 neutron histories.

TABLE 6.4.* Criticality of Gd_2O_3 - Poisoned Plutonium Solution(a)

Concentration - ∿367 g Pu/ℓ
Molarity - ∿4M

Gd Concentration, g Gd/ℓ	Height, inch	Buckling,(b) cm^{-2}
∿4	∿10.4	0.010772
∿5	∿11.0	0.010266
∿6	∿11.7	0.009781
∿8	∿12.9	0.009035
∿10	∿14.2	0.008395
∿13	∿16.2	0.007590
∿16	∿18.4	0.006971
∿19	∿21.1	0.006404
∿21	∿23.3	0.006058

(a) 24 inch diameter, water reflected, cylindrical vessel

(b) λ = 7 cm

* *Preliminary*

The computed criticality factors are listed in Table 6.5, which includes pertinent experimental data on the critical systems. The computed values of k_{eff} are found to display a slight negative bias, departing from unity on the average by about 1.8%. The reasons for the discrepancy are being examined.

A technical paper summarizing these results has been prepared.(1)

1. *R. C. Lloyd, E. D. Clayton, and L. E. Hansen, "Criticality of Plutonium Nitrate Solution Containing Soluble Gadolinium," Transactions, American Nuclear Society, vol. 14, no. 1, June 1971.*

TABLE 6.5. Criticality of Gd_2O_3 - Poisoned Plutonium Solutions[a]

Gd Concentration g Gd/ℓ	Critical Values: Height, cm	Volume, ℓ	Mass, kg Pu	Buckling,[b] cm^{-2}	Computed k_{eff}
0	15.44	45.17	5.240	0.017215	0.993
0.479	20.16	58.98	6.842	0.013651	0.980
0.963	25.98	75.99	8.815	0.010952	0.980
1.420	34.48	100.85	11.698	0.008679	0.978
1.922	48.28	141.24	16.383	0.006826	0.976
2.380	80.37	235.10	27.272	0.005267	0.983

(a) *24-inch diameter, water-reflected, cylindrical vessel*
Chemical analysis - 116 g Pu/ℓ, 1.85 M acid, 238.9 g NO_3/ℓ total, specific gravity = 1.2552
Isotopic analysis (wt%) - ^{238}Pu = 0.44, ^{239}Pu = 90.677, ^{240}Pu - 8.379 ^{241}Pu = 0.851, ^{242}Pu = 0.049

(b) *Buckling computed assuming 7 cm for extrapolation length on vessel's sides and bottom and 5 cm on top*

Criticality of Plutonium Nitrate Solutions Containing Raschig Rings

Raschig rings are being used as neutron absorbers to increase storage capacity of tanks and process vessels and to safe sumps in facilities where plutonium solutions are handled. Experiments have been performed to obtain data for use in establishing criticality safety guidelines and for use in checking calculational models for poisoned systems. These experiments were made using stainless steel vessels (wall thickness 0.031 in.) of 12, 18, and 24-in. diameters, reflected with water. Raschig rings of stainless steel and borosilicate glass rings were used in these experiments. The stainless steel rings were 1/2-in. OD, 1/2-in. long, having a 1/16-in. wall thickness, and contained 1 wt% boron. Two types of glass rings were used, one containing 1/2 wt% boron, the other containing 4 wt% boron. These rings were 1.5-in. OD, 1.25-in. ID and 1.7-in. long.

Plutonium nitrate solutions containing 8.3 wt% ^{240}Pu throughout a concentration range of 63 to 412 g Pu/liter were used in the cylindrical vessels containing the Raschig rings.

Critical approach measurements were used to determine the critical height of the assembly containing the 1/2 wt% B rings, while exponential measurements were used on the other assemblies.

The variation of critical height with plutonium concentration for the 24-in. diameter assemblies containing the 1/2 wt% B rings is shown in Figure 6.1. The critical volume is very sensitive to concentration change in the 60 g Pu/liter region, but is very insensitive in the 200 - 400 Pu/liter range, approaching a minimum between 300 - 400 g Pu/liter. The unpoisoned system would have a minimum in the 175 - 200 g Pu/liter range.

The relationship between critical mass and plutonium concentrations for the assemblies containing the 1/2 wt% B rings is shown in Figure 6.2. A minimum critical mass occurs at about 110 g/liter for these assemblies. This compares to a nonpoisoned system minimum of about 30 g Pu/liter.

Buckling values determined for the assemblies are given in Table 6.6. A water-reflected extrapolation length of 7 cm was assumed for determination of buckling values. The measured volume displaced by the rings is also given in this table.

The 4 wt% B glass rings poisoned the system sufficiently to produce negative bucklings for lower concentrations, but the buckling was positive for the 391 g Pu/liter concentration. The stainless steel rings resulted in negative bucklings for both of the concentrations (275, 412 g/liter) measured.

For systems without rings, the buckling is essentially constant in the 275 - 412 g/liter range; however, the increase in buckling for the more concentrated solution is to be expected in the poisoned systems because of faster neutron spectrum. Boron, being basically a thermal neutron poison, becomes less effective in the faster spectrum, with fewer resultant neutron absorptions in the rings - with consequent higher buckling.

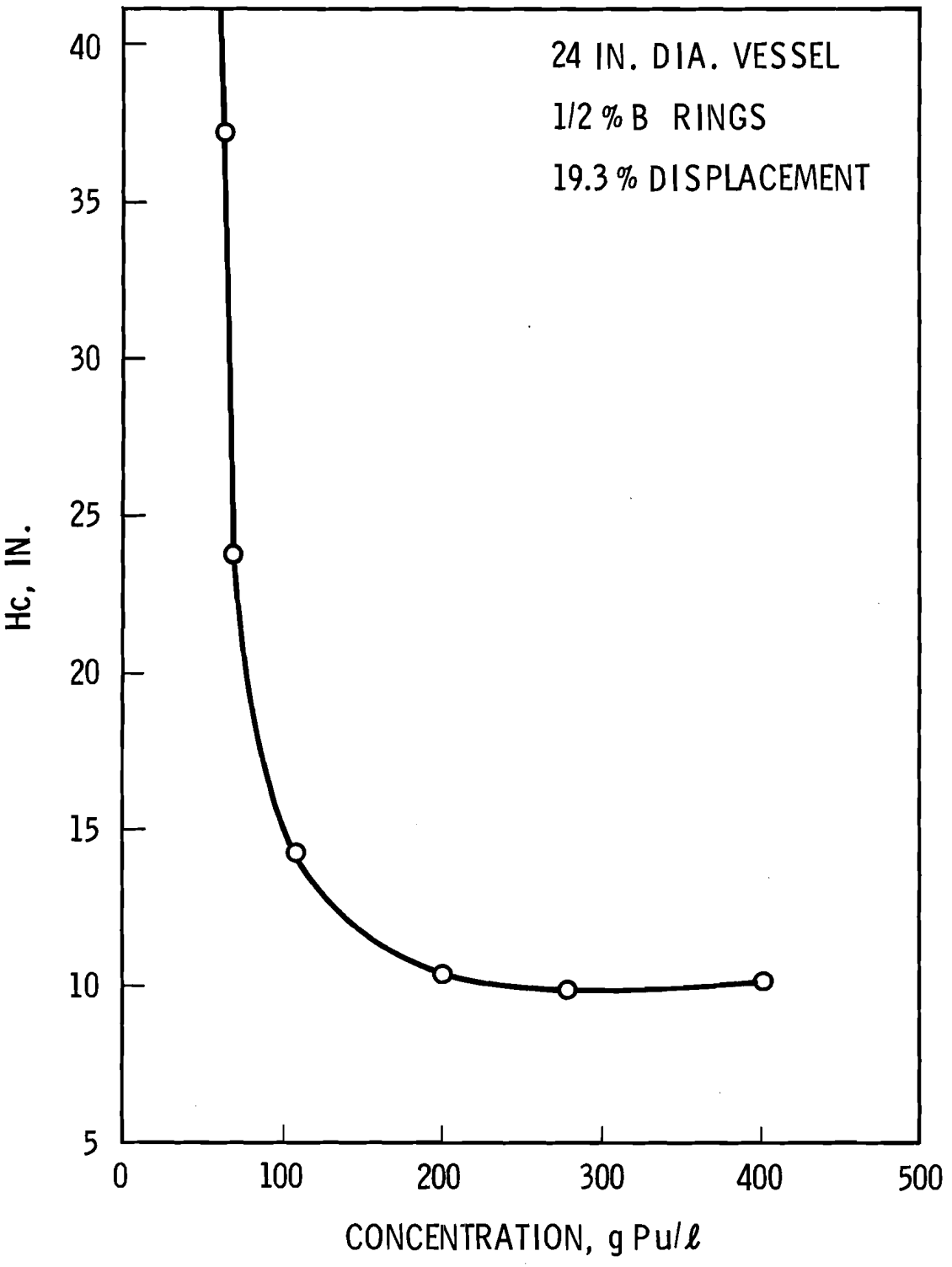

FIGURE 6.1. Raschig Ring Criticality

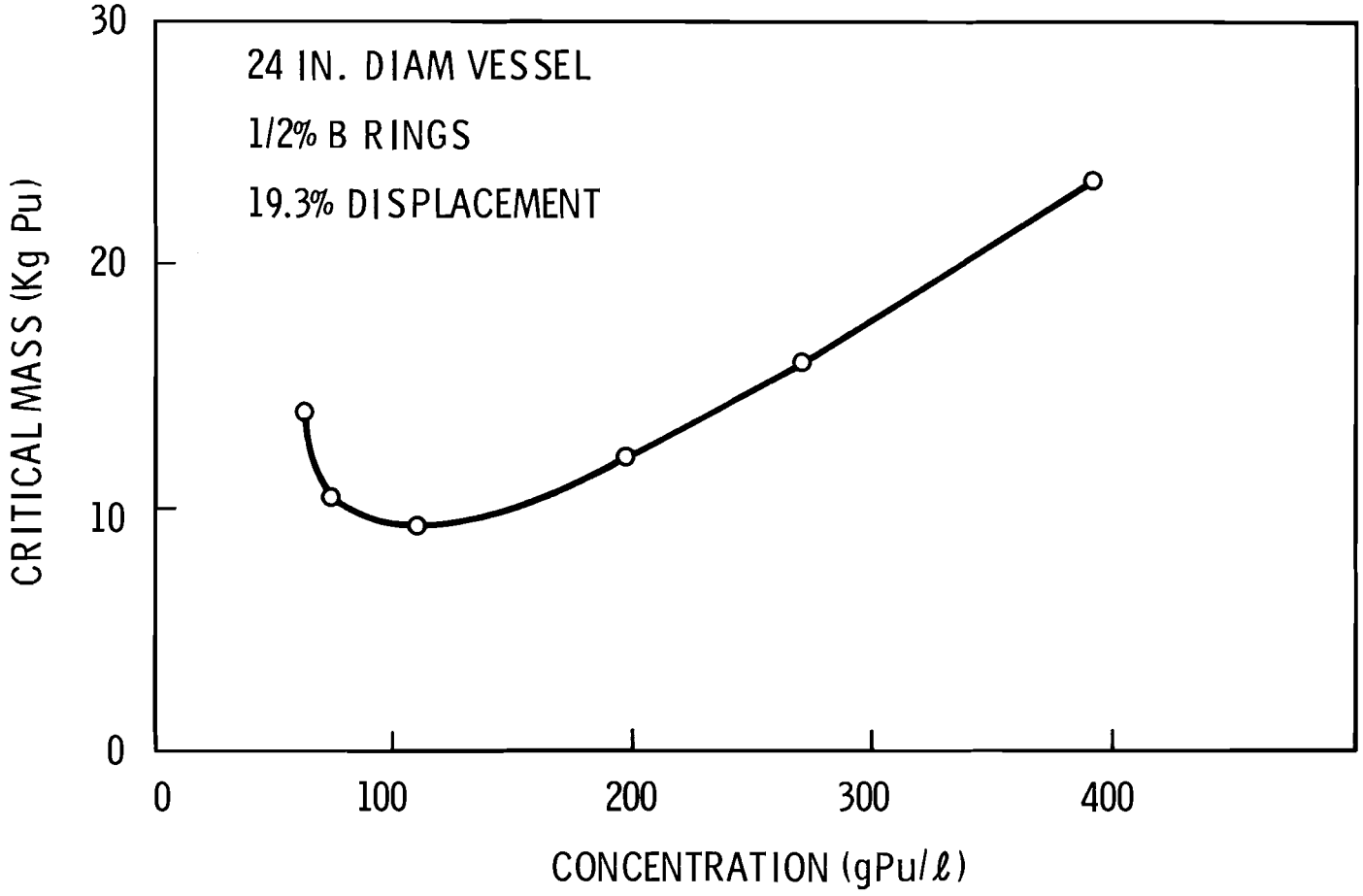

FIGURE 6.2. Effect of Raschig Rings on the Critical Mass of $Pu(NO_3)_4$

TABLE 6.6. Effect of Raschig Rings on Criticality

RASCHIG RINGS				
MATERIAL	BORON CONTENT (%)	VOLUME DISPLACEMENT (%)	SOLUTION CONCENTRATION (g Pu/liter)	BUCKLING (cm^{-2})
GLASS	1/2	19.3	391	0.011135
	1/2	19.3	271	0.011300
	1/2	19.3	197	0.010912
	1/2	19.3	110	0.008462
	1/2	19.3	74	0.006024
	1/2	19.3	63	0.004996
	4	18.78	391	0.002
	4	18.78	271	-0.0006
	4	18.78	121	-0.006
STAINLESS STEEL	1	27	275	-0.011
	1	27	412	-0.006
NONE	0	0	275	0.0176

The KENO multigroup Monte Carlo code was used to calculate k_{eff} values for the experimental critical systems. The results of these calculations are given in Table 6.7. In this analysis it was assumed that the systems were homogeneous. It is seen that the assumption is reasonable for the higher concentrations, but results in a significant underestimation of k_{eff} at the lower concentrations. This is expected, since self-shielding in the Raschig rings will increase as the neutron spectrum becomes softer in the lower concentration solutions. The calculations on homogenized systems will be correlated with calculations on heterogeneous systems, which better describe the experimental system, to heuristically quantize the effects of the self-shielding.

TABLE 6.7. Calculated k_{eff} of Boron - Poisoned Systems

Solution Concentration, g Pu/ℓ	k_{eff}
No Rings	
275	1.0005 ± 0.0090
1/2 wt% B Rings	
391	0.996 ± 0.010
271	0.981 ± 0.008
197	0.983 ± 0.008
110	0.954 ± 0.008
74	0.942 ± 0.007
63	0.929 ± 0.005

7. CALCULATIONS OF POTENTIAL ENVIRONMENTAL RADIOLOGICAL CONSEQUENCES OF REACTOR ACCIDENTS

E. C. Watson

This study has been completed and a Final Report will be issued separately.

8. NUCLEAR GRAPHITE

G. L. Tingey

IN-REACTOR CREEP

W. J. Gray

Molten Salt Reactors require a graphite moderator that maintains its integrity at least up to a fast-neutron fluence of 2.5×10^{22} n/cm^2 (E > 0.18 MeV). High-Temperature Gas-Cooled Reactors, although currently designed so that the moderator is replaced at more frequent intervals, have an economic incentive to extend the lifetime up to a comparable fluence also. In order to be sure that the graphite does not fracture under thermal and irradiation-induced stresses, irradiation-creep behavior at these high fluences must be determined. Low fluence irradiation-creep constants for some graphite types have been determined previously[1] by restraining a sample with a graphite holder of a different type or a different orientation. The complex length-change behavior of graphite, however, renders this type of experiment unsatisfactory at high fluences. Therefore, constant-stress experiments must be performed. Such experiments are currently being conducted by Battelle-Northwest.

Two creep capsules containing graphite samples under compressive stresses are being irradiated at 550 and 800°C. A third creep capsule to contain samples under tensile stresses has been designed and will operate at 800°C. In addition, a fourth creep capsule is planned which will contain samples under compressive stresses and operate at about 1100°C. This capsule is scheduled to be charged into the reactor about September 1971.

The two compressive creep capsules operating at 550°C and 800°C were discharged from the reactor in February 1971 after the second irradiation period. Results are shown in Table 8.1. Within the scatter of the data, the creep is shown to be linear with stress and of about the expected magnitude for the AGOT graphite. For the other two graphites, the creep constants are a little smaller than for most nuclear graphites,[1] but this is not particularly surprising since these graphites are also considerably stronger.

TABLE 8.1. Length Changes of Graphite Under Compressive Stress after Two Irradiation Periods

Graphite	Irradiation Temp, °C	Fluence × 10^{-21} E > 0.18 MeV	Stress, psi	ΔL %	Creep$_1$ Const, × $_{-1}10^{27}$ (psi^{-1}-n/cm^2)$^{-1}$
AGOT	800	6.60	0	-2.30	
		5.68	1000	-2.97	1.49
		6.82	2000	-5.31	2.29
		7.31	3000	-6.08	1.57
	550	6.60	0	-2.71	
		5.68	1000	-2.76	1.36
		6.82	2000	-3.97	0.74
		7.31	3000	-5.37	1.03
H337	800	6.80	0	0.00	
		6.21	1000	-0.65	1.03
		6.92	2000	-1.64	1.11
		7.28	3000	-2.21	0.90
	550	6.80	0	-0.70	
		6.21	1000	-0.98	0.40
		6.92	2000	-1.66	0.55
		7.28	3000	-2.23	0.54
AXF-8QBG1	800	6.76	0	+0.57	
		6.51	1000	-0.38	1.42
		6.87	2000	-0.91	1.12
		7.19	3000	-2.42	1.36
	550	6.51	0	-0.24	
		6.23	1000	-0.58	0.36
		6.87	2000	-1.45	0.85
		6.43	3000	-1.66	0.51

- *Fluences are estimated.*
- *Unstressed length changes are averages of 10 to 20 samples.*
- *Stressed length changes are for one sample (AGOT) or two samples (H337 and 4XF-8QBG1).*

Upon discharging the two creep capsules from the reactor, it was discovered that some of the stressed samples were stuck in their holders. Careful analysis of the situation, however, has shown that only two of the samples (the two AXF-8QBG1 samples under 1,000 psi stress at 800°C) were stuck for more than a brief period, and that stress levels on the other samples were not affected by the two badly stuck samples. Stress levels on these two samples cannot be accurately determined, so their creep constants cannot be considered reliable at this point. It may be that their future creep behavior will have been altered also. Data from the other samples that were evidently stuck only briefly may also be in some doubt at this time, but it is felt that the effect on future behavior will be negligible. Fortunately, several samples are known to have experienced the proper stress levels during the entire irradiation, so the data from these samples can be compared with those from samples that were stuck and the consequences assessed. A comparison of data from stuck and unstuck samples shows no significant differences. This further encourages us to believe that the usefulness of the experiment has not been jeopardized.

The primary goal of the irradiation-creep program is to investigate creep behavior, both compressive and tensile, at very high fluences where rapid expansion occurs in unstressed samples. The determination of low-fluence creep behavior is only of secondary importance. Therefore, we have decided to continue the irradiation of at least one sample for each graphite type and irradiation condition. New samples placed under irradiation now would not reach fluences as high as required without a long extension of the irradiation program. However, two new samples will be placed in each capsule to provide reliable low-fluence data and also to provide a means of evaluating the effect of being "stuck" in the holder on the high-fluence data.

These additional samples can be accommodated in the current capsule design by increasing the portion of space occupied by samples by 2.5 inches. Although the end positions are less favorable for irradiation, the samples will still provide valuable information that would otherwise be lost.

A tensile creep experiment has also been designed, and the samples and capsule parts have been fabricated. A string of dumbbell-shaped samples with threaded ends will be held together by threaded couplings and the stress will be applied by a single bellows. Varied sample cross sections will permit tensile stresses of 1000, 2000, and 3000 psi on the AXF-8QBG1 and H337 graphites and 670, 1330, and 2000 psi on the AGOT graphite. Duplicate samples will be included at 1000 psi for the AXF-8QBG1 and H337 graphites, making a total of 11 samples. These stressed samples, along with a number of unstressed (control) samples, will be irradiated at 800°C.

Since the design of the tensile creep capsule has the disadvantage that the stress would be removed from all the samples if one sample were to break, a warning system has been incorporated to notify the operation when a sample breaks. In such an event, the reactor would be shut down and the capsule discharged immediately.

Initial measurements are currently being made on the tensile creep samples. These will be charged into the ETR in July 1971 for a one-cycle irradiation. At the same time, the two compressive creep capsules will be charged for a three-cycle irradiation. Necessary changes are being made to insure that the problem of samples sticking in the holders does not recur.

RADIOLYTIC REACTIONS IN GRAPHITE MODERATED REACTORS

G. L. Tingey and R. P. Turcotte

The radiolytic reaction of carbon monoxide and water vapor is under investigation as part of a continuing study of the effects of helium dilution on coolant chemistry in the HTGR system. The initial results obtained for the case $[H_2O] = [CO] = 940$ ppm, [He] = 1 atm are shown in Figure 8.1, plotted as $\ln (G/T^{1/2})$ versus 1/RT to give equations in the form:

$$75 < T°C < 650 \quad G_{CO_2} = 0.162\ T^{1/2}$$

$$75 < T°C < 310 \quad G_{H_2} = 0.055\ T^{1/2}$$

$$310 < T < 650 \quad G_{H_2} = 0.463\ T^{1/2}\ e^{-2500/RT}$$

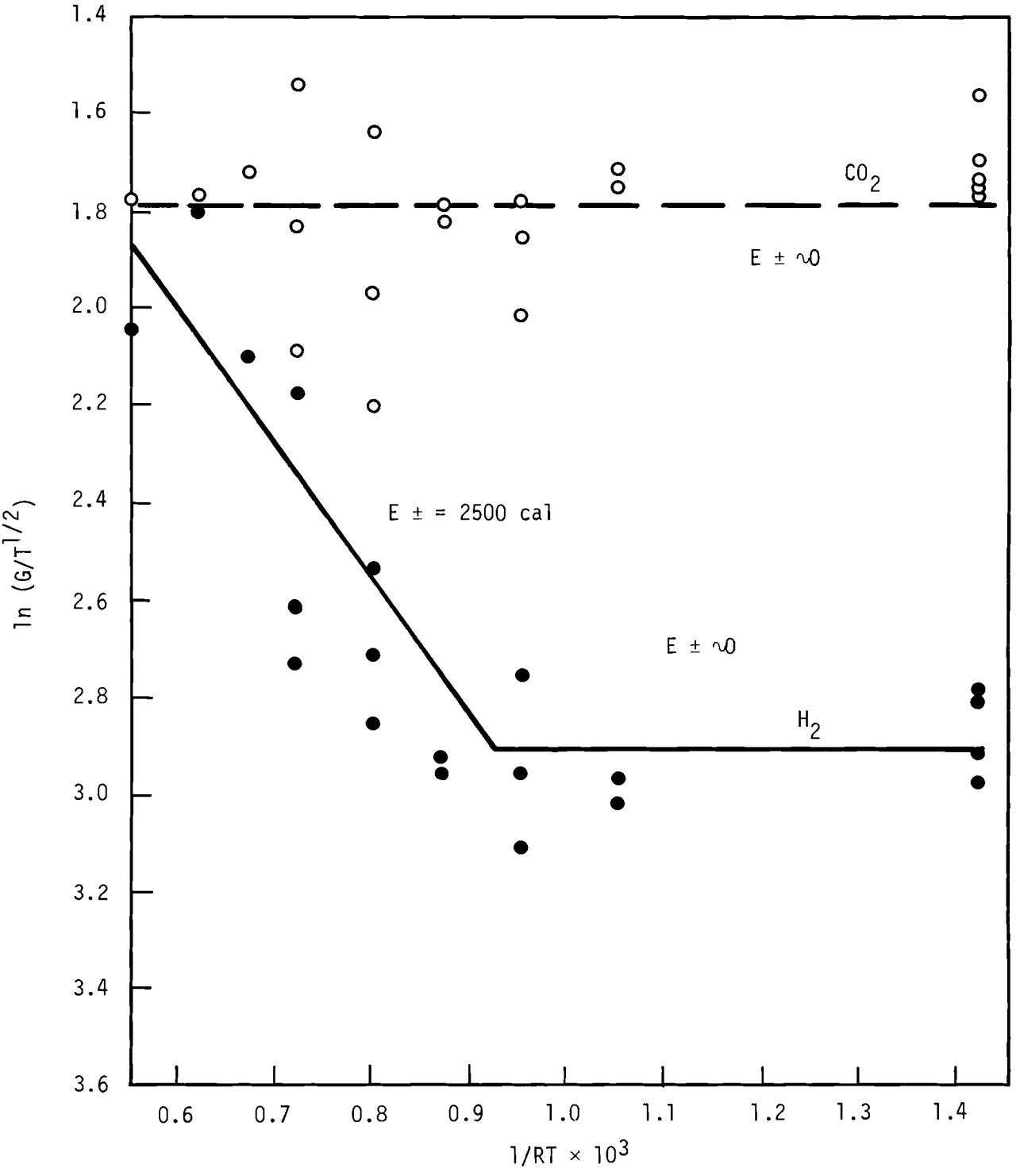

FIGURE 8.1. Radiolysis of a Gaseous Mixture of CO and H_2O as a Function of Temperature

These results suggest a quite different behavior than obtained for the undiluted gases[2] ([CO] = [H_2O] = 0.5 atm), where the activation energy obtained for CO_2 was 800 cal below 300°C and 2500 cal between 300 and 500°C. For H_2, E ± 2500 cal for 100-500°C was obtained. A large reduction in activation energy with increasing dilution has been previously reported[3] for the H_2 + CO_2 reaction, so the near zero values obtained in the present case for CO_2 are possible.

The change noted for H_2 at approximately 270° is remarkable, but the overall high degree of scatter needs to be reduced to accurately define the behavior of this system. In this respect, some modifications have been made to enable better control of H_2O partial pressure and to facilitate dilution of the reactant gases to lower concentrations. The kinetic data will be evaluated in terms of effects on the HTGR system via the GOP computer simulation program.

EFFECT OF SAMPLE SIZE ON DIMENSIONAL STABILITY OF GRAPHITE

W. J. Gray

There is ample evidence which shows that the irradiation behavior of large graphite bars as used in reactor construction is significantly different from that of small samples normally tested in irradiation programs.[4] Initially the difference in behavior was attributed merely to sample size differences. Controlled irradiation of large samples failed to show the large differences previously observed.[5] This task was therefore undertaken to gain an understanding of those factors which contribute to the apparent size effect.

Two different experimental approaches to this problem are currently being taken. The first involves the irradiation of a large number of samples of various sizes and shapes in the Hanford KE-reactor to investigate the effect of factors associated only with sample size. The second involves a phenomenon called "cold-seeding" wherein the graphite samples are irradiated briefly at low temperatures prior to the normal high

temperature irradiation. Several samples which have been previously cold-seeded are currently being irradiated to high fluences at high temperatures in the ETR.

Due to the shutdown of the KE-reactor, about one-fourth of the size-effect samples being irradiated therein have recently been discharged. Physical difficulties have prevented removal of all the samples. Discharged samples have been measured and the data are currently being evaluated. The experiment will be discontinued because of the reactor shutdown. However, the samples have a total fluence of about 3×10^{21} n/cm^2 ($E > 0.18$ MeV) at this time, and it should be possible to quantitatively ascertain the effect of sample size on contraction rates.

The cold-seeding capsule was discharged from the ETR in March 1971, rather than May 1971, as was originally planned, because it was felt that a smaller exposure increment would be desirable. Peak fluences for these samples are now about 3×10^{21} n/cm^2 ($E > 0.18$ MeV). Those cold-seeded samples found to be contracting at a significantly different rate than unseeded samples will be irradiated for a third exposure beginning about August 1971.

HIGH TEMPERATURE IRRADIATIONS

W. J. Gray and W. C. Morgan

The first of the larger size, high-temperature irradiation capsules was discharged from the ETR at the end of Cycle 110B, in March. This irradiation brings some of the samples to a fluence of about 1.8×10^{22} n/cm^2 ($E > 0.18$ MeV). Measurement of the samples began in April, and it is planned that the next capsule will be charged in the ETR during August 1971.

MECHANISM OF IRRADIATION DAMAGE

W. C. Morgan and W. J. Gray

Bulk thermal expansion and radiation-induced dimensional changes of polycrystalline aritificial graphites are both[6] dependent on (a) the

changes occurring in the crystallites, (b) the orientation of crystallites within the body, (c) the morphology of oriented porosity relative to the crystalline regions and (d) effects arising from other phenomena, such as stresses and changes in the non-graphitic carbon component. Of these, (c) and (d) are not directly measurable at the present time and must be obtained from analysis of the bulk changes and a knowledge of items (a) and (b). Although the thermal expansion of graphite single crystals has been measured, the measurements are not sufficiently precise to satisfy the requirements for an analysis of bulk changes. Therefore, we have attempted to improve the precision through an analysis of available data, using the theoretical relationships derived by Riley.[7]

Characteristic Debye lattice vibration temperatures, of $\theta_a = 800 \pm 10°C$ and $\theta_c = 2300 \pm 10°C$, were derived from measured specific heat data over the range 150°K to 1800°K. Using Riley's extension[7] of the Gruneisen and Goens[8] theory on the relationship between thermal expansion, elastic moduli and heat capacities of hexagonal crystals, the available lattice thermal expansion coefficients were fitted to equations of the form:

$$\alpha_a = A\, C_{v_a} + B\, C_{v_c} + CT$$

$$\alpha_c = L\, C_{v_a} + M\, C_{v_c} + NT$$

$$\ln \frac{a}{a_o} = A\, U_a + B\, U_C + \frac{C}{2} T^2$$

$$\ln \frac{c}{c_o} = L\, U_a + M\, U_c + \frac{N}{2} T^2$$

where α_a and α_c are the crystal lattice thermal expansion coefficients, respectively, parallel and transverse to the crystal basal planes;

a and a_o are the crystal lattice a-spacings at temperature T and at °K respectively;

c and c_o are the respective lattice c-spacings;

A, B, C, L, M and N are treated as constants;

$C_{v_a} = 3\ R\ D\ (\frac{\theta_a}{T})$ and $C_{v_c} = 3\ R\ D\ (\frac{\theta_c}{T})$ are the contributions to the crystal specific heat by lattice vibrations parallel and transverse to the basal planes;

$$U_a = 3\ RT\ F\ (\frac{\theta_a}{T}) \text{ and } U_c = 3\ RT\ F\ (\frac{\theta_c}{T})$$

and the Debye functions $D\ (\frac{\theta}{T})$ and $F\ (\frac{\theta}{T})$ have been numerically evaluated and tabulated by Beattie.[9]

Best fits of the theoretical equations to the available data were obtained with the coefficients:

$$a_o = 2.4617\ \text{Å}$$
$$A = 0.7023 \times 10^{-6}\ \text{mole/cal}$$
$$B = -0.4337 \times 10^{-6}\ \text{mole/cal}$$
$$C = -0.830 \times 10^{-10}\ \text{deg}^{-2}$$
$$c_o = 3.341\ \text{Å}$$
$$L = -3.320 \times 10^{-6}\ \text{mole/cal}$$
$$M = 6.512 \times 10^{-6}\ \text{mole/cal}$$
$$N = 0.7187 \times 10^{-8}\ \text{deg}^{-2}$$

Riley's equations, relating the crystal elastic moduli to the above equations for lattice thermal expansion coefficients and heat capacities, can be expressed in the form:

$$(s_{11} + s_{12}) = AK/2\ (A + L + x)$$
$$s_{13} = LK/4\ (A + L + x)$$
$$s_{33} = xK/(A + L + x)$$

where s_{11}, s_{12}, s_{13}, and s_{33} are the usual crystal elastic moduli, A, B, L, and M are the coefficients, $x = ML/4B$, and K is the volumetric compressibility.

K can be written in terms of the linear compressibilities parallel (K_a) and transverse (K_c) to the crystal basal planes:

$$K = 2\,K_a + K_c$$

$$K_a = s_{11} + s_{12} + s_{13}$$

$$K_c = 2\,s_{13} + s_{33}$$

The compressibilities are not independently obtainable from the theoretical equations; however, if one uses the value, $K = 29.6 \times 10^{-13}$ cm^2/dyne, recomputed by Gschneidner[10] from the high pressure measurements of Bridgman,[11] one obtains the elastic moduli and compressibilities shown and compared with previous evaluations in Table 8.2.

TABLE 8.2. Elastic Moduli and Compressibilities of a Graphite Single Crystal

(In unit of 10^{-13} cm^2/dyne)

	This Analysis	Spence[b]	Seldin[c]	Other
$s_{11} + s_{12}$	1.05	1.06	0.82	
s_{13}	-2.49	-2.49	-0.33	
s_{33}	37.4	33.2	27.5	
K_a	-1.44	-1.43	+0.49	
K_c	32.4	28.2	26.8	28.6[d]
K	-(a)-	26.3	27.8	

a. *Using $K = 29.6 \times 10^{-13}$ cm^2/dyne as given by Gschneidner.*[10]
b. *Review of previous data, see Reference 12.*
c. *Recent measurements on stress-annealed pyrolytic graphite, see Reference 13.*
d. *Measurements by Kabalkina and Vereshchagin, Reference 14.*

The very close agreement of the derived values for $(s_{11} + s_{12})$, s_{13} and K_a, with the best values given by Spence must be considered fortuitous; a smaller assumed value for K would result in lower numbers for all

quantities derived from this analysis. However, the agreement with previous evaluations is considered excellent and lends strong support to the validity of using Riley's theoretical equations, with the derived coefficients, to describe the crystal lattice expansion as a function of temperature.

The next phase of this investigation will be aimed at obtaining information on the morphology of the oriented porosity relative to the crystalline regions in polycrystalline graphites by analysis of the bulk thermal expansion as a function of temperature, using these derived equations for the thermal expansion of component crystallites. It is currently accepted[15] that the oriented porosity exerts the same influence on the radiation-induced dimensional changes as it does on the thermal expansion.

Subsequent phases of this investigation will probe more deeply into the effect of oriented porosity on the bulk changes and the variation in oriented porosity as a function of neutron fluence.

References

1. *R. Blackstone, L. W. Graham, and M. R. Everett. "High Temperature Radiation Induced Creep in Graphite," paper presented at the 9th Carbon Conference, Boston, Mass., June 1969.*
2. *G. L. Tingey. "Radiolysis of Mixtures of Carbon Monoxide and Water Vapor," HW-SA-3440. Available from the National Technical Information Service, Springfield, VA. April 1964.*
3. *"Technical Activities Quarterly Report, AEC Reactor Development and Technology Programs, July, August, September 1970," BNWL-1522-1. Battelle-Northwest, Richland, Washington, October 1970.*
4. *W. J. Gray. "Summary of the Size-Effect Phenomenon in Graphite Irradiations," May 22, 1970 (Classified Internal Report).*
5. *W. J. Gray. "The Effect of Sample Size on the Irradiation-Induced Contraction of Nuclear Graphite," presented at the Ninth Biennial Conference on Carbon, June 16-20, 1969.*
6. *W. C. Morgan. Carbon, vol. 4, p. 215. 1966.*
7. *D. P. Riley. Proc. Phys. Soc. (London), vol. 57, p. 486. 1945.*
8. *E. Gruneisen and E. Goens. Z. Phys., vol. 29, p. 141. 1924.*
9. *J. A. Beattie. J. Math. Phys., vol. 6, p. 1. 1926.*
10. *K. A. Gschneidner, Jr. Solid State Physics, vol. 16, p. 275, Academic Press, New York. 1965.*

11. P. W. Bridgman. Daedalus, vol. 76, p. 9. 1945.

12. G. B. Spence. Proc. Fifth Conf. on Carbon, vol. 2, Pergamon Press, London, 1962.

13. E. J. Seldin. "Summary Papers - Ninth Biennial Conference on Carbon," The Defense Ceramic Information Center, Columbus, Ohio. 1969.

14. S. S. Kabalkina and L. F. Vereshchagin, translated in Soviet Physics "Doklady," vol. 5, p. 373. 1960.

15. W. C. Morgan. J. Appl. Phys., vol. 38, p. 1996. 1967.

9. ATR PRESSURIZED WATER LOOP OPERATION AND MAINTENANCE

R. S. Hope

The Advanced Test Reactor began Cycle 5 startup on September 13, 1970. Cycle 5 ended on October 19, 1970 after accumulating an exposure of 6826.8 MWd or 31.03 effective days at 220 MW. Cycle 6 started operation on November 1, 1970 and completed the cycle on January 12, 1971. Accumulated exposure was 10,328.0 MWd or 46.945 effective days at 220 MW. Cycle 7 startup began January 20, 1971 and was completed March 14, 1971. Accumulated exposure was 9909.5 MWd or 45.04 effective days at 220 MW. The reactor is still shut down in preparation for Cycle 8A startup now scheduled for April 8, 1971.

The 1D-N loop was operated during Cycles 5 and 6 at 2000 psig, 520°F, 45 gpm, PH 10.00 ± 0.2 with oxygen concentration at less than 0.05 ppm. The loop test train contained zircaloy-2 corrosion coupons sponsored by DUN (Douglas United Nuclear) and stainless steel structural materials sponsored by NRL (Navy Research Labs). The loop test train was charged out for Cycle 7 and operating conditions were changed to 2200 psig, 560°F inlet water temperature and 40 gpm flow. The PH and oxygen concentration remained the same. The new test train contained 56 inches of vion and stainless steel structural specimens from the NRL. The same sample train, except for ten small resonance fatigue specimens, will be irradiated during Cycle 8.

The zircaloy corrosion coupons removed from the loop test train after Cycle 6 were weighed and examined in the NRTS hot cell. The samples were then shipped to the WADCO hot cell at Richland, Washington on January 31, 1971. Two sets of stainless steel samples, each 14 inches long, were also shipped to NRL in Washington, D.C. on February 2, 1971.

One hundred sixty-eight miniature tensile specimens which had been discharged from the 1D-N loop test train after Cycle 5 on October 19, 1970 were shipped to the WADCO hot cell at Richland, Washington on February 10, 1971.

Because AEC-RDT funding for the ATR Water Loop Operation and Maintenance program ends June 30, 1971, Battelle-Northwest has transferred the 1D-N loop and associated equipment to Idaho Nuclear Corporation. This will be the last quarterly report on this program.

10. PUBLICATIONS AND PRESENTATIONS

DOCUMENTS PUBLISHED

E. A. Aitken, S. K. Evans, and D. C. Wadekamper, "Behavior of Discrete PuO_2 Particles in a Thermal Recycle Fuel During SPERT Power Transients", NEDG-12146, November 1970.

DOCUMENTS IN PUBLICATION

E. P. Lippincott, Derivation of Corrections to k_∞ in the Two-Group Approximation, BNWL-1560, (1971).

R. I. Smith, J. W. Kutcher, J. H. Lauby, and L. D. Williams, Critical Experiments with the UO_2 - 2 wt% PuO_2 Batch Core in the PRTR, BNWL-1553, January 1971.

ACCEPTED FOR PUBLICATION

S. R. Bierman and E. D. Clayton, "Critical Experiments with Unmoderated PuO_2," BNWL-SA-4030, accepted for publication in the July issue of Nuclear Technology.

E. D. Clayton, "Criticality Control and Safety (of Transuranium Elements)," BNWL-SA-3746, to be published in Gmelin's Handbook der Anorganischen Chemie, vol. 71; Transuranium Elements.

E. D. Clayton and S. R. Bierman, "Criticality Problems of Actinide Elements," BNWL-SA-3449, to be published in Actinides Reviews.

D. A. Kottwitz, "Parallel Beams of Neutrons or X-Rays by Multiple Bragg Reflection," GNWL-SA-3784, submitted to Acta Crystallographica, January 1972.

JOURNAL ARTICLES SUBMITTED

J. K. Bahl and M. D. Freshley, "Plutonium and Fission Product Migration in Mixed Oxide Fuels During Migration in Mixed-Oxide Fuels During Irradiation," BNWL-SA-3441, December 1970. Submitted to Nuclear Technology.

M. D. Freshley, "A Comparison of Pellet and Vipac Nuclear Fuels," BNWL-SA-3466, July 1970, submitted to Journal of Nuclear Engineering and Design.

M. D. Freshley, "Operation with Center Melting," BNWL-SA-3461, July 1970, submitted to Journal of Nuclear Engineering and Design.

C. R. Richey, "Determination of Neutron Multiplication Factors as a Function of Temperature with the HTLTR," BNWL-SA-3689. Submitted to Nuclear Science and Engineering.

T. J. Oakes, "Measurement of the Neutron Multiplication Factor as a Function of Temperature for a $^{235}UC_2$-$^{232}ThO_2$-C Lattice," BNWL-SA-3621. Submitted to Nuclear Science and Engineering.

A. D. Vaughn, "Fuel Rod Enrichment Determination by Gamma Ray Spectrometry."

M. D. Freshley, E. A. Aitken, D. C. Wadekamper, R. L. Johnson, and W. G. Lussie, "Behavior of Discrete PuO_2 Particles in Mixed-Oxide Fuel During Rapid Power Transients," BNWL-SA-3443, January 1971, Submitted to Nuclear Technology.

PRESENTATIONS

J. K. Bahl and M. D. Freshley, "Plutonium and Fission Product Migration in Mixed-Oxide Fuels During Irradiation," BNWL-SA-3441; also Trans. Am. Nucl. Soc., vol. 13 (2), 1970.

M. D. Freshley, E. A. Aitken, D. C. Wadekamper, R. L. Johnson, and W. G. Lussie, "Behavior of Discrete PuO_2 Particles in Thermal Recycle Fuel During Rapid Power Transients," BNWL-SA-3443; also Trans. Am. Nucl. Soc., vol. 13 (2), 1970.

J. M. Neill and D. L. Prezbindowski, "Uncertainties in Predicting Thermal Spectra and Lattice Multiplications for Al-5 wt% Pu Fuel Light Water Systems, BNWL-SA-3653-A, to be published in Trans. Third. Conf. on Neutron Cross Sections and Technology, Knoxville, Tenn., March 15-17, 1971.

B. R. Leonard, Jr., and Duane H. Thomsen, "The Effect of Incident Neutron-Energy Dependent Fission-Neutron Spectra on Fast-Reactor Calculations," to be published in Transactions Third Conference on Neutron Cross Sections and Technology, Knoxville, Tenn., March 15-17, 1971.

U. P. Jenquin, "Sensitivity of a Plutonium-Fueled Burnup Experiment to Microscopic Cross-Section Data," BNWL-SA-3658-A, to be published in Transactions Third Conference on Neutron Cross Sections and Technology, Knoxville, Tenn., March 15-17, 1971.

R. C. Lloyd and E. D. Clayton, "Criticality of Plutonium Nitrate Solutions Containing Raschig Rings," BNWL-SA-3447; also Trans. Am. Nucl. Soc., vol. 13, (2), November 1970.

C. L. Brown and C. A. Rogers, "Critical Approach and Exponential Experiments with Prototype FFTF Driver Pins in Water," BNWL-SA-3501; also Trans. Am. Nucl. Soc., vol. 13, (2), November 1970.

ACCEPTED FOR PRESENTATION

1971 Annual Meeting of the American Nuclear Society, Boston, Massachusetts, June 13-17, 1971.

John M. Allen, Kermit L. Garlid and E. Duane Clayton, "Source-Jerk Determination of Subcritical Reactivity Using a Californium-252 Source," BNWL-SA-3770-S.

R. C. Lloyd, E. D. Clayton and L. E. Hansen, "Criticality of Plutonium Nitrate Solution Containing Soluble Gadolinium," BNWL-SA-3769-S.

S. R. Bierman and E. D. Clayton, "Critical Experiments with Mixed Oxides of Pu and U Containing 30 and 15 wt% Plutonium," BNWL-SA-3695-S.

D. L. Prezbindowski and R. P. Matsen, "Physics of Burnup and Plutonium Fuels in Thermal Reactors," BNWL-SA-3777-A.

V. O. Uotinen, W. P. Stinson, S. P. Singh, "β_{eff}/ℓ in a Pu-Enriched H_2O Lattice Containing Water Regions,' BNWL-SA-3755.

E. P. Lippincott, "Temperature Dependence of k_∞ for a ThO_2-$^{233}UO_2$ HTGR Lattice," BNWL-SA-3756.

DISTRIBUTION

No. of Copies

OFFSITE

2 AEC Chicago Patent Group
- G. H. Lee

10 AEC Division of Reactor Development and Technology
- Asst. Dir. for Project Management
- Chief, Water Project Branch (2)
- Chief, Gas Cooled Projects Branch
- Asst. Dir. for Reactor Technology
- Chief, Reactor Physics Branch (2)
- Chief, Core Design Branch
- Chief, Fuels and Materials Branch (2)

1 AEC Division of Nuclear Materials Safeguards
- H. Werner

1 AEC Division of International Affairs
- M. B. Kratzer

1 AEC Division of Materials Licensing
- R. J. Odegaarden

1 AEC Division of Production
- F. P. Baranowski

3 AEC Division of Reactor Licensing
- R. E. Baker
- R. E. Ireland
- P. A. Morris

1 AEC Division of Research
- G. A. Kolstad

215 AEC Division of Technical Information Extension

1 AEC Savannah River Operations Office
- R. Thorne

No. of Copies

6 Argonne National Laboratory

Reactor Physics Constants Center (2)
R. Avery
C. H. Bean
P. Gast
R. E. Macherey

5 Atomic Energy of Canada Limited
Chalk River, Ontario, Canada

D. H. Charlesworth
M. Duret
C. Millar
L. Pease
H. K. Rae

2 Atomic Energy Establishment
Dragon Project
Winfrith, Dorchester,
Dorset, England

M. R. Everett
H. Gutmann

3 Atomic International

H. Alter
N. Ketzlach
Liquid Metals Engineering Center (LMEC)

1 Australian Atomic Energy Commission
AAEC Research Establishment
Private Mail Bag, Sutherland 2232
N.S.W., Australia

Dr. J. L. Symonds
Chief, Physics Division

1 Battelle Memorial Institute
Columbus, Ohio

Roger Merrill

3 Babcock and Wilcox Company
161 E. 42nd Street
New York, N. Y. 10017

H. M. Jones
D. H. Roy
W. A. Wittkopf

No. of Copies	
1	Bechtel Corporation Vernon, California M. Aronchick
1	Bettis Laboratory, Westinghouse Electric Company J. J. Taylor
2	Bhabha Atomic Research Centre Trombay, Bombay-85, India S. R. Dwivedi, Theoretical Physics Section/RED Central Complex Bldg. J. K. Bahl, Metallurgy Division Modular Laboratories
3	Brookhaven National Laboratory J. Chernick H. Kouts S. Pearlstein
1	Mr. H. B. Brooks 310 Power Bldg. Chattanooga, Tennessee 37401
1	California Institute of Technology H. Lurie, Engineering Div.
1	Catholic University of America Dept. of Nuclear Sci. & Eng. Washington, D.C. G. L. Simmons
10	C.E.N. - Saclay Boite Postale 2 Gif-Sur-Yvette (S et 0), France B. LaPonche P. Lecorche G. Vendryes
1	CNEN - Casaccia 00060 - S. Maria Di Galeria Rome, Italy Paolo Loizzo

No. of Copies

2 CNEN-Centro Studi-Nucleaire
Casaccia, Rome, Italy

Ugo Farinelli
Augusto Gandini

3 Combusion Engineering, Nuclear Division

W. P. Chernock
R. Harding
S. Visner

2 Cornell University, Ithaca, N.Y.

R. T. Cuykendall, Eng. Physics
M. Nelkin

2 Assoc. C.E.N. Belgo Nucleaire
35 Rue Des Colonies, Belgium

H. Bairiot
L. Bindler

2 Duke University
Durham, N.C.

H. W. Newson, Physics Dept.
W. J. Seeley, School of Eng.

1 Ebasco Services

D. R. de Boisblanc

3 Edison Electric Institute
750 Third Avenue
New York, N.Y. 10017

John J. Kearney (2)
George Watkins

6 E. I. du Pont de Nemours & Co., Inc.,
Savannah River Laboratory

H. K. Clark
J. L. Crandall
G. Dessauer
E. J. Hennelly
H. Honeck
J. Suich

No. of Copies	
1	ENEL Via G. B. Martini (Pizaaz Verdi) Rome, Italy Mr. Paoletti Gualandi
10	EURATOM 53, Rue Billiard Brussels 4, Belgium A. de Stordeur
1	FFR - AB Atomenergi Studsvik, Pa NYKOPING Sweden Evelyn Sokolowski
4	General Atomic R. C. Dahlberg J. M. Neill H. B. Stewart G. D. Trimble
3	General Electric Company Knolls Atomic Power Laboratory R. Ehrlich C. Lubitz K. W. Seeman
7	General Electric Company San Jose R. L. Crowther M. R. Egan D. L. Fischer P. Greebler S. Levy R. B. Richards T. M. Snyder
1	General Electric Company Nucleonics Laboratory H. W. Alter
2	General Electric Company Vallecitos Atomic Laboratory B. F. Judson T. M. Snyder

No. of Copies

5 Gulf General Atomic

W. E. Bell
R. F. Turner
Moffett
W. V. Goeddel
G. B. Engle

2 Idaho Nuclear Corporation
P. O. Box 1845
Idaho Falls, Idaho 83401

R. M. Brugger
R. A. Grimesey

1 Istanbul Technical University
Giimiis, Suyer, Istanbul, Turkey

Director, Nuclear Energy Institute

1 Japan Atomic Energy Research Institute (JAERI)
Tokaimura, Naka-gun, Ibarakiken, Japan

Hjime Sakata

1 Japan Atomic Energy Institute (JPDR-TCA)
Tokaimura, Ibarakiken, Japan

Shojiro Matsuura

1 Kansas State University
Manhattan, Kansas

W. R. Kimel, Nuclear Eng.

1 Kernforschungszentrum Karlsruhe
7500 Karlsruhe, Germany

Professor W. Haefele

1 Kerr-McGee
Oklahoma City, Oklahoma

Dr. Frank Pittman

2 Los Alamos Scientific Laboratory

G. E. Hansen
M. C. Smith

No. of Copies

1 Manhattan College
Riverdale, New York, N.Y.
Brother Gabriel Kane

2 Massachusetts Institute of Technology
Professor Irving Kaplan
D. D. Lanning

1 North American Aviation Science Center
E. R. Cohen

1 North Carolina State College
R. L. Murray

1 Nuclear Fuels Services, Inc.
Suite 906
Wheaton Plaza Bldg.
Wheaton, Maryland 20902
R. E. L. Stanford

2 Nuclear Materials and Equipment Corp.
Apollo, Pennsylvania
C. S. Caldwell
Karl Puechl

1 NUKEM
D-645, NANAU
POSTFACH 869
Germany
Mr. Wolgang K. L. Jager

6 Oak Ridge National Laboratory
J. H. de Nordwell
W. P. Eatherly
R. R. Kasten
F. C. Maienschein
A. M. Perry
M. W. Rosenthal

1 Pakistan Institute of Nuclear Science & Technology
P. O. Nilore, Rawalpindi, Pakistan
M. A. Manna

No. of Copies

1 Penn State College
W. F. Witzig

1 Pennsylvania State University
University Park, Pennsylvania
P. L. Walker

1 Philadelphia Electric Company
1000 Chestnut Street
Philadelphia 5, Pa.
Wayne C. Astley

1 Phillips Petroleum Company
Idaho Falls, Idaho
W. B. Lewis

1 Power Reactor and Nuclear Fuel Development Corp.
9-13, 1-chome, Akasaka
Minato-ku, Tokyo, Japan
Setsuo Kobayashi

1 Purdue University
P. N. Powers, Nucl. Eng. Dept.

1 Rensselaer Polytechnic Institute
E. R. Gaerttner

1 S. C. K. - C. E. N.
BRL,
Mol-Donk, Belgium
Dr. H. Vanden Broeck

1 Tennessee Valley Authority
310 Power Bldg., Chattanooga, Tenn.
H. B. Brooks

1 Union Carbide Corporation (ORNL)
E. B. Johnson

No. of Copies

2 United Kingdom Atomic Energy Agency
Atomic Weapons Research Establishment
Aldermaston, Berkshire, UK

R. C. Lane (1)

Authority Health and Safety Branch,
Safeguards Division, Risley,
Warrington, UK

J. H. Chalmers (1)

2 United Kingdom Atomic Energy Authority
Atomic Energy Research Establishment - Harwell
Didcot, Berkshire, England

J. H. W. Simmons
John Wright

2 United Kingdom Atomic Energy Authority
General Reactor Physics Division
Winfrith, England

Dr. J. G. Tyror
C. G. Campbell

1 United Nuclear Corporation
Elmsford, N.Y. 10523

J. R. Tomonto

1 United Nuclear Corporation

T. B. Holden

1 University of Arizona
Tucson, Arizona

Monte V. Davis, Nucl. Eng. Dept.

1 University of California
Department of Nuclear Engineering

V. E. Schrock

1 University of Florida
Gainesville, Florida

R. E. Uhrig, Nucl. Eng.

1 University of Illinois
Urbana, Illinois

Frederick Seitz, Physics Dept.

No. of Copies	
1	University of London Reactor Silwood Park, Sunninghill, Ascot, Berkshire, England D. MacMahon
1	University of Minnesota Minneapolis, Minnesota H. S. Isben, Chem. Eng. Dept.
1	University of Nevada Reno, Nevada T. V. Frazier, Physics Dept.
1	University of Notre Dame Notre Dame, Indiana E. W. Jerger, Dept. of Mech. Eng.
1	University of Oregon Eugene, Oregon J. L. Powell, Physics Dept.
2	University of Tennessee Knoxville, Tennessee A. H. Nielsen, Physics Dept. P. F. Pasqua, Nucl. Eng. Dept.
1	University of Toledo Toledo, Ohio J. J. Turin
3	University of Washington Seattle, Washington A. L. Babb, Dept. of Nucl. Eng. D. G. Fischbach K. L. Garlid
1	University of Wisconsin Madison 6, Wisconsin M. W. Carbon, Nucl. Eng. Com.
1	U. S. Atomic Energy Commission DNR A. Radkowsky

No. of Copies

1 Virginia Polytechnic Institute
Blacksburg, Virginia

A. Robeson, Physics Dept.

1 Washington State University
Pullman, Washington

J. P. Spielman, Col. of Eng.

10 Westinghouse Electric Corporation

C. A. Anderson
R. J. French
W. D. Leggett
R. S. Miller
P. M. Murray
R. E. Olsen
W. L. Orr
J. Haley
J. R. Worden
J. H. Wright

1 Whiteshell Nuclear Research Establishment
Atomic Energy of Canada, Ltd.
Pinawa, Manitoba, Canada

R. B. Lyon, Head-Assessment and Applied Math. Section

ONSITE-HANFORD

1 AEC Chicago Patent Group

R. M. Poteat

5 AEC Richland Operations Office

H. A. House (2)
C. L. Robinson (2)
M. R. Schneller

7 Atlantic Richfield Hanford Company

S. J. Beard
R. D. Carter
R. E. Isaacson
G. R. Kiel
A. E. Smith
R. E. Tomlinson
ARHCO File

No. of Copies

2 Computer Sciences Corporation

E. Z. Block
R. J. Shields

1 Donald W. Douglas Laboratories

J. Greenborg

17 Douglas United Nuclear

T. W. Ambrose
G. F. Bailey
C. E. Bowers
P. A. Carlson
G. C. Fullmer
L. L. Grumme
R. O. Gumprecht
J. P. Hamric
C. D. Harrington
C. W. Kuhlman
R. H. Meichle
R. Nilson
W. S. Nechodom
G. F. Owsley
DUN File (3)

6 RDT Assistant Director for Pacific Northwest Programs

W. E. Fry
P. G. Holsted (2)
J. B. Kitchen
D. W. Mazur
T. A. Nemzek

21 WADCO

E. T. Boulette
W. L. Bunch
J. J. Cadwell
J. A. Christensen
E. A. Evans
R. E. Heineman
P. L. Hofmann
R. L. Junkins
W. W. Little
R. E. Peterson
C. A. Rogers
R. E. Schenter
W. F. Sheeley
R. C. Smith
B. Wolfe
K. L. Young
WADCO Document Control (5)

No. of Copies

124 Battelle-Northwest

F. W. Albaugh
C. A. Bennett
C. L. Bennett
S. R. Bierman
C. L. Brown
S. H. Bush
G. J. Busselman
D. G. Carter
J. L. Carter
N. E. Carter
T. D. Chikalla
D. E. Christensen
R. G. Clark
E. D. Clayton
G. M. Dalen
L. C. Davenport
E. C. Davis
F. G. Dawson (10)
T. F. Demmitt
D. E. Deonigi
R. L. Dillon
J. R. Divine
B. H. Duane
J. B. Edgar
G. W. R. Endres
P. L. Farnsworth
L. G. Faust
L. G. Federico
J. W. Finnigan
J. R. Fishbaugher
H. A. Fowler
J. C. Fox
M. D. Freshley
J. J. Fuquay
G. L. Gelhaus
A. G. Gibbs
S. Goldsmith
R. L. Gulley
V. W. Gustafson
C. E. Haines
R. J. Hall
L. E. Hansen
G. E. Hanson
O. K. Harling
W. M. Harris
C. M. Heeb

No. of
Copies

Battelle-Northwest (contd)

H. L. Henry
R. J. Hoch
R. H. Holeman
R. S. Hope (BNW, Idaho Falls)
U. P. Jenquin
B. M. Johnson
R. D. Johnson
R. A. Kennedy
G. J. Konzek
D. A. Kottwitz
J. W. Kutcher
C. R. Lagergren
D. D. Lanning
J. H. Lauby
D. C. Lehfeldt
B. R. Leonard, Jr.
D. L. Lessor
W. R. Lewis
R. C. Liikala
C. W. Lindenmeier
E. P. Lippincott
R. C. Lloyd
R. P. Matsen
G. C. Moore
D. F. Newman
R. E. Nightingale
T. J. Oakes
D. R. Oden, Jr.
L. T. Pederson
H. M. Parker
R. S. Paul
W. W. Porath
D. L. Prezbindowski
R. H. Purcell
W. L. Purcell
W. A. Reardon
C. R. Richey
W. D. Richmond
W. C. Roesch
J. T. Russell
G. L. Schiefelbein
L. C. Schmid (6)
G. D. Seybold
R. I. Smith
K. B. Stewart
W. P. Stinson
H. J. Svoboda, Jr.
D. H. Thomsen
G. L. Tingey
V. O. Uotinen
A. D. Vaughn
W. P. Walsh
L. D. Williams
N. G. Wittenbrock
W. C. Wolkenhauer
D. C. Worlton
F. R. Zaloudek
M. G. Zimmerman
Technical Publications (1)
Technical Information (5)